

RESEARCH ARTICLE | JUNE 16 2025

Large-scale clustering of inertial particles in a rotating, stratified and inhomogeneous turbulence

Nathan Kleeorin; Igor Rogachevskii  



Physics of Fluids 37, 065152 (2025)

<https://doi.org/10.1063/5.0270977>



Articles You May Be Interested In

Planetesimal Formation Induced by Sintering

AIP Conf. Proc. (August 2009)

Gravitational instabilities in protostellar discs and the formation of planetesimals

AIP Conf. Proc. (June 2010)

Experimental study of turbulent transport of nanoparticles in convective turbulence

Physics of Fluids (May 2022)



Physics of Fluids
Special Topics
Open for Submissions

[Learn More](#)

Large-scale clustering of inertial particles in a rotating, stratified and inhomogeneous turbulence

Cite as: Phys. Fluids **37**, 065152 (2025); doi: [10.1063/5.0270977](https://doi.org/10.1063/5.0270977)

Submitted: 14 March 2025 · Accepted: 28 April 2025 ·

Published Online: 16 June 2025



View Online



Export Citation



CrossMark

Nathan Kleeorin^{1,2} and Igor Rogachevskii^{1,3,a)} 

AFFILIATIONS

¹Department of Mechanical Engineering, Ben-Gurion University of the Negev, P. O. Box 653, Beer-Sheva 84105, Israel

²IZMIRAN, Troitsk, 108840 Moscow Region, Russia

³Nordita, KTH Royal Institute of Technology and Stockholm University, Hannes Alfvéns väg 12, SE-10691 Stockholm, Sweden

^{a)}Author to whom correspondence should be addressed: gary@bgu.ac.il. URL: <http://www.bgu.ac.il/~gary>

ABSTRACT

We develop a theory of various kinds of large-scale clustering of inertial particles in a rotating density stratified or inhomogeneous turbulent fluid flows. The large-scale particle clustering occurs in scales that are much larger than the integral scale of turbulence, and it is described in terms of the effective pumping velocity in a turbulent flux of particles. We show that for a fast rotating strongly anisotropic turbulence, the large-scale clustering occurs in the plane perpendicular to rotation axis in the direction of the fluid density stratification. We apply the theory of the large-scale particle clustering for explanation of the formation of planetesimals (progenitors of planets) in accretion protoplanetary disks. We determine the radial profiles of the radial and azimuthal components of the effective pumping velocity of particles which have two maxima corresponding to different regimes of the particle–fluid interactions: at the small radius it is the Stokes regime, while at the larger radius it is the Epstein regime. With the decrease in the particle radius, the distance between the maxima increases. This implies that smaller-size particles are concentrated near the central body of the accretion disk, while larger-size particles are accumulated far from the central body. The dynamic time of the particle clustering is about $\tau_{\text{dyn}} \sim 10^5$ – 10^6 years, while the turbulent diffusion time is about 10^7 years, which is much larger than the characteristic formation time of large-scale particle clusters ($\sim \tau_{\text{dyn}}$).

© 2025 Author(s). All article content, except where otherwise noted, is licensed under a Creative Commons Attribution (CC BY) license (<https://creativecommons.org/licenses/by/4.0/>). <https://doi.org/10.1063/5.0270977>

I. INTRODUCTION

Turbulent transport of particles has been investigated in a number of publications due to various applications in geophysics, astrophysics, as well as in turbulent industrial flows.^{1–8} Particular interest is related to transport of particles by rotating turbulence in astrophysical flows (e.g., formation of planetesimals as progenitors of planets in protoplanetary disks^{9–14}) as well as in geophysical flows (e.g., dynamics of particles in the atmospheric tornado and duststorms¹⁵).

The key phenomena in particle turbulent transport include small-scale particle clustering and large-scale particle clustering. Small-scale clustering arises in scales that are much smaller than the integral turbulence scale. On the other hand, the large-scale particle clustering (i.e., formation of large-scale inhomogeneous spatial distributions in particle number density) occurs in scales that are much larger than the integral scale of turbulence.

Typical examples of the large-scale particle clustering are turbophoresis due to particle inertia and inhomogeneity of turbulence^{16–19} and turbulent thermal diffusion in temperature stratified turbulence.^{20,21} Turbophoresis results in the accumulation of inertial particles in the vicinity of the minimum of the turbulent intensity, while turbulent thermal diffusion causes the formation of large-scale particle clusters in the vicinity of the mean temperature minimum.

Turbulent thermal diffusion has been intensively investigated analytically^{20–27} using different theoretical approaches. This effect has been found in direct numerical simulations,^{28–30} detected in various laboratory experiments,^{31–35} studied in geophysical,³⁶ and planetary³⁷ turbulence as well as in astrophysical turbulence.¹²

In the present theoretical study, we show that the rotation results in various types of large-scale clustering of inertial particles in density stratified or inhomogeneous turbulent fluid flows. For fast rotating strongly anisotropic turbulence, the dominant contribution to the

large-scale clustering occurs in the plane perpendicular to rotation axis in the direction of the fluid density stratification. The developed theory of large-scale particle clustering is applied for an explanation of the formation of planetesimals (progenitors of planets) in accretion protoplanetary disks.

This paper is organized as follows. In Sec. II, we discuss general ideas for developing a mean-field theory describing the turbulent transport of inertial particles in a rotating turbulence. Here, we present a general expression for effective pumping velocity of particles in density stratified and inhomogeneous rotating turbulence. In Sec. III, we outline the method of derivations and approximations made to determine the rotational contributions to the Reynolds stress and the turbulent heat flux. This allows us to derive expressions for various contributions to the effective pumping velocity of particles describing different kinds of large-scale particle clustering in small-scale density stratified and inhomogeneous rotating turbulence. In Sec. IV, we discuss applications of the analyzed effects for formation of planetesimals in protoplanetary disks. Finally, conclusions and discussions are given in Sec. V. In Appendix A, we derive expression for the total effective pumping velocity of inertial particles, while in Appendix B we obtain the rotational contributions to the Reynolds stress and the turbulent heat flux. In Appendix C, we give the identities used for the derivation of the total effective pumping velocity of inertial particles.

II. PARTICLES IN A ROTATING TURBULENCE

Equation for the number density $n_p(t, r)$ of small particles advected by a random fluid flow reads

$$\frac{\partial n_p}{\partial t} + \text{div}(n_p \mathbf{V}) = D \Delta n_p, \quad (1)$$

where D is the coefficient of molecular (Brownian) diffusion, \mathbf{V} is a random velocity field of particles which they acquire in a turbulent fluid velocity \mathbf{u} in a low-Mach-number flow. Note that $\text{div} \mathbf{V} \neq 0$ is due to particle inertia and inhomogeneity of the fluid density.^{10,20,38}

Now, we consider the large-scale dynamics of inertial particles in a fast rotating turbulent fluid flow. The equation for the mean field $\bar{n} = \langle n_p \rangle$ derived using different analytical approaches^{8,20,21} reads

$$\frac{\partial \bar{n}}{\partial t} + \text{div} [\bar{n} \mathbf{V}^{\text{eff}} - \hat{\mathbf{D}}^T \nabla \bar{n}] = D \Delta \bar{n}, \quad (2)$$

where the first term in the squared brackets of Eq. (2), $\bar{n} \mathbf{V}^{\text{eff}}$, determines the contribution to the turbulent flux of particles caused by the effective pumping velocity. This effective pumping velocity is given by

$$\mathbf{V}^{\text{eff}} = -\langle \tau \mathbf{V} \text{div} \mathbf{V} \rangle, \quad (3)$$

where τ is the turbulent correlation time of the fluid flow. The second term, $-\hat{\mathbf{D}}^T \nabla \bar{n} = -D_{ij}^T \nabla_j \bar{n}$, in the squared brackets of Eq. (2) determines the contribution to the flux of particles caused by turbulent diffusion, and

$$D_{ij}^T = \langle \tau V_i V_j \rangle \quad (4)$$

is the turbulent diffusion tensor. We consider particles advected by a rotating turbulent fluid flow for large Péclet numbers and large Reynolds numbers. The equation of motion for particles is given by

$$\frac{d\mathbf{V}}{dt} = \frac{\mathbf{u} - \mathbf{V}}{\tau_p} + 2\mathbf{V} \times \boldsymbol{\Omega}, \quad (5)$$

where \mathbf{V} is the random velocity field of particles caused by fluctuations of the fluid velocity \mathbf{u} , which are determined by equation

$$\frac{d\mathbf{u}}{dt} = -\frac{\nabla P}{\bar{\rho}} + \nu \Delta \mathbf{u} + 2\mathbf{u} \times \boldsymbol{\Omega} + \frac{\mathbf{f}}{\bar{\rho}}. \quad (6)$$

Here, $\boldsymbol{\Omega}$ is the angular velocity, P is fluid pressure fluctuations, $\bar{\rho}$ is the mean fluid of the density, ν is the kinematic viscosity, \mathbf{f} is the external random force, and τ_p is the stopping time describing particle and fluid interaction. The notion “stopping” time is originated in astrophysics.

When the mean-free path of the gas molecules is much smaller than the particle radius, the particle and fluid interaction is described by the Stokes regime with $\tau_p = m_p / (6\pi \bar{\rho} \nu a_p) = 2\rho_p a_p^2 / (9\bar{\rho} \nu)$, where ρ_p is the material density of particles, and m_p and a_p are the particle mass and the particle radius, respectively. In the opposite case, when the mean-free path of the gas molecules is larger than the particle radius, the stopping time τ_p is determined by the Epstein regime with $\tau_p = \rho_p a_p / (\bar{\rho} c_s)$,^{9,11,13,14} where c_s is the sound speed.

Equation (5) can be rewritten as

$$A_{ij} V_j = u_i - \tau_p \frac{dV_i}{dt}, \quad (7)$$

where $A_{ij} = \delta_{ij} - \omega \varepsilon_{ijk} \hat{\Omega}_k$, $\hat{\Omega} = \boldsymbol{\Omega} / \Omega$ is the unit vector, ε_{ijk} is the fully anti-symmetric Levi-Civita unit tensor, δ_{ij} is the symmetric Kronecker unit tensor and $\omega = 2\tau_p \Omega$. Multiplying Eq. (7) by the inverse matrix

$$A_{mi}^{-1} = \frac{1}{1 + \omega^2} (\delta_{mi} + B_{mi}), \quad (8)$$

we obtain

$$\mathbf{V}_m = \frac{1}{1 + \omega^2} (\delta_{mi} + B_{mi}) \left[u_i - \tau_p \frac{dV_i}{dt} \right], \quad (9)$$

where $B_{mi} = \omega (\varepsilon_{mis} \hat{\Omega}_s + \omega \hat{\Omega}_m \hat{\Omega}_i)$ and $A_{mi}^{-1} A_{in} = \delta_{mn}$. By means of Eq. (9), we determine $\text{div} \mathbf{V}$ which characterizes a compressibility of particle velocity field caused by the particle inertia, inhomogeneous fluid density, and rotation

$$\begin{aligned} \text{div} \mathbf{V} = \text{div} \mathbf{u} + \frac{1}{1 + \omega^2} & \left[\omega (\hat{\Omega} \cdot \text{rot} \mathbf{u} - \omega \text{div} \mathbf{u}_\perp) \right. \\ & \left. - \text{div} \left(\tau_p \frac{d\mathbf{V}}{dt} \right) - \nabla_m \left(\tau_p B_{mi} \frac{dV_i}{dt} \right) \right], \end{aligned} \quad (10)$$

where the fluid velocity \mathbf{u}_\perp is in a plane perpendicular to $\boldsymbol{\Omega}$. To derive Eq. (10), we use the identity $B_{mi} \nabla_m = \omega (\boldsymbol{\Omega} \times \nabla)_i + \omega^2 \hat{\Omega}_i (\hat{\Omega} \cdot \nabla)$.

There are three characteristic times in the system: the stopping time describing particle–fluid interaction τ_p , the correlation turbulent time τ_0 in the integral scale ℓ_0 , and the period of rotation $t_\Omega = 2\pi/\Omega$. These three times are independent of each other. In the developed theory, there are two independent parameters: $\omega = 2\tau_p \Omega$ and $\Omega_s = 4\Omega \tau_0$. The stopping time τ_p is the smallest time in the system. The case $\tau_p \ll \tau_0 \ll \Omega^{-1}$ corresponds to a slow rotation ($\Omega \tau_0 \ll 1$), while the case $\tau_p < \Omega^{-1} \ll \tau_0$ corresponds to a fast rotation ($\Omega \tau_0 \gg 1$). For small time τ_p (in comparison with τ_0), we apply a method of iterations.

Using expression for the tensor B_{mi} and applying a method of iterations for small time τ_p , Eqs. (9) and (10) are transformed to Eqs. (A3) and (A11) (see for details Appendix A). Using Eqs. (A3) and

(A11), we determine the total effective pumping velocity: $\mathbf{V}^{(\text{eff})} = -\langle \tau \mathbf{V} \text{div} \mathbf{V} \rangle$, which is given by

$$\mathbf{V}^{(\text{eff})} = \mathbf{V}^{(A)} + \hat{\boldsymbol{\Omega}} \times \mathbf{V}^{(B)} + \hat{\boldsymbol{\Omega}} (\hat{\boldsymbol{\Omega}} \cdot \mathbf{V}^{(C)}), \quad (11)$$

where

$$\mathbf{V}^{(A)} = \frac{1 + 3\omega^2}{(1 + \omega^2)^4} \left[(1 + 3\omega^2) \mathbf{V}^{(1)} + (1 - \omega^2) \right. \\ \left. \times (\omega^2 \mathbf{V}^{(2)} + \mathbf{V}^{(3)}) - \omega^2 (3 + \omega^2) \mathbf{V}^{(4)} + 2\omega^3 \mathbf{V}^{(5)} \right], \quad (12)$$

$$\mathbf{V}^{(B)} = -\frac{2\omega^3}{(1 + \omega^2)^4} \left[(1 + 3\omega^2) \mathbf{V}^{(1)} - \omega^2 (1 - \omega^2) \mathbf{V}^{(2)} \right. \\ \left. + (1 + 5\omega^2 + 2\omega^4) \mathbf{V}^{(3)} - \omega^2 (3 + \omega^2) \mathbf{V}^{(4)} + 2\omega^3 \mathbf{V}^{(5)} \right], \quad (13)$$

$$\mathbf{V}^{(C)} = -\frac{\omega^2 (1 - \omega^2)}{(1 + \omega^2)^4} \left[(1 + 3\omega^2) (\mathbf{V}^{(1)} + \mathbf{V}^{(3)}) \right. \\ \left. - \omega^2 (\mathbf{V}^{(2)} + \mathbf{V}^{(4)}) + 2\omega^3 \mathbf{V}^{(5)} \right], \quad (14)$$

and the effective velocities $\mathbf{V}^{(k)}$ describing various kinds of large-scale particle clustering are given by

$$\mathbf{V}^{(1)} = -\langle \tau \mathbf{u} \text{div} \mathbf{u} \rangle, \quad (15)$$

$$\mathbf{V}^{(2)} = -\langle \tau \mathbf{u} (\hat{\boldsymbol{\Omega}} \cdot \nabla) (\hat{\boldsymbol{\Omega}} \cdot \mathbf{u}) \rangle, \quad (16)$$

$$\mathbf{V}^{(3)} = -\frac{\tau_p}{\bar{\rho}} \langle \tau \mathbf{u} \Delta P \rangle, \quad (17)$$

$$\mathbf{V}^{(4)} = -\frac{\tau_p}{\bar{\rho}} \langle \tau \mathbf{u} (\hat{\boldsymbol{\Omega}} \cdot \nabla)^2 P \rangle, \quad (18)$$

$$\mathbf{V}^{(5)} = -\langle \tau \mathbf{u} (\hat{\boldsymbol{\Omega}} \cdot \text{rot} \mathbf{u}) \rangle. \quad (19)$$

III. LARGE-SCALE EFFECTS

In this section, we derive the expressions for the effective velocities $\mathbf{V}^{(k)}$ defined by Eqs. (15)–(19). We take into account the effect of rotation on turbulence. In particular, to derive equation for the rotational contributions to the Reynolds stress and the turbulent heat flux, we follow the approach developed in Refs. 39 and 40. We use equations for fluctuations of velocity \mathbf{u}' and entropy $s' = \theta/\bar{T} - (1 - \gamma^{-1})P/\bar{P}$

$$\frac{\partial \mathbf{u}'}{\partial t} = -\nabla \left(\frac{P}{\bar{\rho}} \right) - \mathbf{g} s' + 2\mathbf{u}' \times \boldsymbol{\Omega} + \mathbf{u}'^N, \quad (20)$$

$$\frac{\partial s'}{\partial t} = -(\mathbf{u}' \cdot \nabla) \bar{s} + S^N, \quad (21)$$

where P and θ are fluctuations of fluid pressure and temperature, respectively, γ is the ratio of specific heats, and \mathbf{g} is the acceleration due to the gravity. The hydrostatic nearly isentropic basic reference state is defined by $\nabla \bar{P} = \bar{\rho} \mathbf{g}$, where \bar{T} , \bar{P} , \bar{s} , and $\bar{\rho}$ are the mean fluid temperature, pressure, entropy, and density, respectively, in the basic reference state. In Eqs. (20) and (21), $\mathbf{u}'^N = \langle (\mathbf{u}' \cdot \nabla) \mathbf{u}' \rangle - (\mathbf{u}' \cdot \nabla) \mathbf{u}'$ and $S^N = \langle (\mathbf{u}' \cdot \nabla) s' \rangle - (\mathbf{u}' \cdot \nabla) s'$ are the nonlinear terms, and the angular brackets imply ensemble averaging. In Eqs. (20) and (21), we neglect small molecular viscosity and heat conductivity terms. Equation (20) is written in the reference frame rotating with the constant angular velocity

$\boldsymbol{\Omega}$. The equations for fluctuations of velocity and entropy are obtained by subtracting equations for the mean fields from the corresponding equations for the total velocity and entropy fields. The fluid velocity for a low Mach number flows with strong inhomogeneity of the fluid density $\bar{\rho}$ is assumed to be satisfied with the continuity equation written in the anelastic approximation $\text{div}(\bar{\rho} \mathbf{u}') = 0$.

To study the effects of rotation on developed density stratified inhomogeneous turbulence, we perform the derivations that include the following steps.

- Using new variables for fluctuations of velocity $\mathbf{U} = \sqrt{\bar{\rho}} \mathbf{u}'$ and entropy $s = \sqrt{\bar{\rho}} s'$;
- Derivation of the equations for the second-order moments of the velocity fluctuations $\langle U_i U_j \rangle$ and the entropy fluctuations $\langle s^2 \rangle$ in the \mathbf{k} space;
- Application of the multi-scale approach⁴¹ that allows us to separate turbulent scales from large scales;
- Adopting the spectral τ approximation^{42–44} (see Appendix B);
- Solution of the derived second-order moment equations in the \mathbf{k} space; and
- Returning to the physical space to obtain expression for the Reynolds stress and turbulent heat flux as the functions of the rotation rate $\boldsymbol{\Omega}$. The details of derivations are discussed in Appendix B.

This procedure allows us to determine the rotational contributions to the Reynolds stress and the turbulent heat flux and to derive expressions for the effective pumping velocities $\mathbf{V}^{(k)}$ of inertial particles in rotating inhomogeneous or density stratified turbulence. The latter describes various kinds of the large-scale particle clustering.

To introduce anisotropy of turbulent velocity field in the background turbulence caused by a fast rotation, we consider an anisotropic turbulence as a combination of a three-dimensional isotropic turbulence and two-dimensional turbulence in the plane perpendicular to the rotational axis. The degree of anisotropy ε_u is defined as the ratio of turbulent kinetic energies of two-dimensional to three-dimensional motions [see Eq. (B19) in Appendix B].

The anisotropy parameter ε_u appeared in the model of the background turbulence depends on the Coriolis number $\text{Co} = 2\Omega\tau_0 = \Omega_*/2$, where τ_0 is the correlation time in the integral scale of turbulence. For a slow rotation (small Coriolis numbers), the parameter $\varepsilon_u \rightarrow 0$. For a fast rotation (large Coriolis numbers), the parameter $\varepsilon_u \gg 1$. In this case, the background turbulence is a highly anisotropic nearly two-dimensional turbulence, and the main rotational contributions to the Reynolds stress are from the two-dimensional part of turbulence. Formally, in the present study when we consider a fast rotating turbulence, the parameter ε_u is not specified (it is a free parameter), but it should satisfy the conditions $\varepsilon_u \gg 1$ for a fast rotation. This phenomenological parameter can be determined, e.g., from DNS or laboratory experiments.

A. The effective pumping velocity $\mathbf{V}^{(1)}$ in inhomogeneous and density stratified turbulence

We determine the effective pumping velocity $\mathbf{V}^{(1)} = -\langle \tau \mathbf{u} \text{div} \mathbf{u} \rangle$ that is given by Eq. (A14) in Appendix A. For slow rotation ($\Omega_*^2 \ll 1$), the effective velocity $\mathbf{V}^{(1)}$ is given by

$$\mathbf{V}^{(1)} = -\lambda D_T + \frac{1}{3} \Omega_* \left[\hat{\boldsymbol{\Omega}} \times \left(\lambda_{\perp} - \frac{1}{2} \mathbf{v}_{\perp} \right) \right] D_T, \quad (22)$$

and for fast rotation ($\Omega_*^2 \gg 1$), it is given by

$$\mathbf{V}^{(1)} = -\frac{3D_T}{4} \lambda_{\perp}, \quad (23)$$

where $D_T = \tau_0 \langle u^2 \rangle / 3$ is the coefficient of turbulent diffusion, $\mathbf{V}_{\perp} = \mathbf{V} - \hat{\Omega} \cdot \mathbf{V}$, $\lambda = -\bar{\rho}^{-1} \nabla \bar{p}$, $\lambda_{\perp} = \lambda - \hat{\Omega} \cdot \lambda$, and $\Omega_* = 4\Omega \tau_0$.

It follows from Eqs. (22) and (23) that in a density stratified turbulence there is a pumping effect of non-inertial particles to the turbulent region with maximum mean fluid density. This effect results in the accumulation of non-inertial particles in the vicinity of the maximum of the mean fluid density. For a non-rotating turbulence, this phenomenon was studied in Ref. 21. The increase in the rotation rate increases the anisotropy of turbulence, and fast rotation causes the effective pumping velocity to be directed in the plane perpendicular to the rotation axis.

The physics of the accumulation of non-inertial particles in the vicinity of the maximum of the mean fluid density can be explained as follows (see, e.g., book⁸). Let us assume that the mean fluid density $\bar{\rho}_2$ at point 2 is larger than the mean fluid density $\bar{\rho}_1$ at point 1. Consider two small control volumes “a” and “b” located between these two points, and let the direction of the local turbulent velocity in volume “a” at some instant be the same as the direction of the mean fluid density gradient $\nabla \bar{p}$ (i.e., along the x -axis toward point 2). Let the local turbulent velocity in volume “b” at this instant be directed opposite to the mean fluid density gradient (i.e., toward point 1).

In a fluid flow with a non-zero mean fluid density gradient, one of the sources of particle number density fluctuations, $n' \propto -\tau_0 \bar{n} (\mathbf{V} \cdot \mathbf{u})$, is caused by a non-zero $\mathbf{V} \cdot \mathbf{u} \approx -\mathbf{u} \cdot \nabla \ln \bar{p} \neq 0$. Since fluctuations of the fluid velocity \mathbf{u} are positive in volume “a” and negative in volume “b,” we have the negative divergence of the fluid velocity, $\mathbf{V} \cdot \mathbf{u} < 0$, in volume “a,” and the positive divergence of the fluid velocity, $\mathbf{V} \cdot \mathbf{u} > 0$, in volume “b.” Therefore, fluctuations of the particle number density $n' \propto -\tau_0 \bar{n} (\mathbf{V} \cdot \mathbf{u})$ are positive in volume “a” and negative in volume “b.” However, the flux of particles $n' u_x$ is positive in volume “a” (i.e., it is directed toward point 2), and it is also positive in volume “b” (because both fluctuations of fluid velocity and number density of particles are negative in volume “b”). Therefore, the mean flux of particles $\langle n' \mathbf{u} \rangle$ is directed, as is the mean fluid density gradient $\nabla \bar{p}$, toward point 2. This results in formation large-scale heterogeneous structures of non-inertial particles in regions with a mean fluid density maximum.

B. The effective pumping velocity $\mathbf{V}^{(2)}$

We determine the effective pumping velocity $\mathbf{V}^{(2)} = -\langle \tau \mathbf{u} (\hat{\Omega} \cdot \mathbf{V}) \times (\hat{\Omega} \cdot \mathbf{u}) \rangle$ that is given by Eq. (A15) in Appendix A. For slow rotation ($\Omega_*^2 \ll 1$), the effective velocity $\mathbf{V}^{(2)}$ is given by

$$\mathbf{V}^{(2)} = \frac{1}{4} \left[2\lambda_{\perp} + \hat{\Omega} (\hat{\Omega} \cdot \mathbf{V}) + \frac{16}{15} \Omega_* \left[\hat{\Omega} \times \left(\lambda_{\perp} - \frac{1}{2} \mathbf{V}_{\perp} \right) \right] \right] D_T, \quad (24)$$

and for fast rotation ($\Omega_*^2 \gg 1$), it is given by

$$\mathbf{V}^{(2)} = -\frac{3\pi}{8\varepsilon_u} \left[\hat{\Omega} \times \left(\lambda_{\perp} - \frac{1}{2} \mathbf{V}_{\perp} \right) \right] D_T, \quad (25)$$

where ε_u is the degree of anisotropy of turbulent velocity field which is large ($\varepsilon_u \gg 1$) for fast rotation $\Omega_* \gg 1$, and it is small for slow

rotation ($\Omega_*^2 \ll 1$). Since for fast rotation $\Omega_* \gg 1$, the degree of anisotropy ε_u of turbulent velocity field is large ($\varepsilon_u \gg 1$), the effective pumping velocity $\mathbf{V}^{(2)}$ vanishes.

C. The effective pumping velocity $\mathbf{V}^{(3)}$

We determine the effective pumping velocity $\mathbf{V}^{(3)} = -\langle \tau_p / \bar{p} \rangle \times \langle \tau \mathbf{u} \Delta P \rangle$ for inertial particles. We consider a low-Mach-number flow, $\text{Ma} = u/c_s \ll 1$, where c_s is the sound speed. For a low-Mach-number fluid flow, the turbulent fluid mass flux $\langle \rho' \mathbf{u} \rangle$ is very small, i.e., it is of the order of Ma^2 , and fluctuations of the fluid density ρ' and velocity \mathbf{u} are weakly correlated. We use the equation of state for a perfect gas, which yields

$$\frac{P}{\bar{P}} = \frac{\rho'}{\bar{\rho}} + \frac{\theta}{\bar{T}} + O(\rho' \theta), \quad (26)$$

and $\langle P \mathbf{u} \rangle / \bar{P} = \langle \theta \mathbf{u} \rangle / \bar{T}$, where we neglect very small turbulent fluid mass flux $\langle \rho' \mathbf{u} \rangle$ for a low-Mach-number flow. Here, \bar{P} , \bar{T} , and $\bar{\rho}$ are the mean fluid pressure, temperature, and density, respectively. Therefore, the effective pumping velocity for inertial particles is

$$\mathbf{V}^{(3)} = -\frac{\tau_p}{\bar{p}} \langle \tau \mathbf{u} \Delta P \rangle \approx -\frac{\tau_p \bar{P}}{\bar{p} \bar{T}} \langle \tau \mathbf{u}(\mathbf{x}) [\nabla^2 \theta(\mathbf{x})] \rangle. \quad (27)$$

Let us determine the correlation function $\langle \tau \mathbf{u}(\mathbf{x}) [\nabla^2 \theta(\mathbf{x})] \rangle$

$$\begin{aligned} \langle \tau \mathbf{u}(\mathbf{x}) [\nabla^2 \theta(\mathbf{x})] \rangle &= \lim_{\mathbf{x} \rightarrow \mathbf{y}} \langle \tau \mathbf{u}(\mathbf{x}) [\nabla^2 \theta(\mathbf{y})] \rangle \\ &= - \int \tau(k) k^2 \langle \mathbf{u}(\mathbf{k}) \theta(-\mathbf{k}) \rangle^{(\Omega)} d\mathbf{k}, \end{aligned} \quad (28)$$

where the correlation function $\langle u_i(\mathbf{k}) \theta(-\mathbf{k}) \rangle^{(\Omega)}$ in the \mathbf{k} space follows from Eq. (B24). Using Eqs. (B24) and (B25) given in Appendix B and Eqs. (27) and (28), we determine the effective pumping velocity $\mathbf{V}^{(3)}$, that is given by Eq. (A16) in Appendix A. For slow rotation, $\Omega_*^2 \ll 1$, the effective pumping velocity $\mathbf{V}^{(3)}$ is given by

$$\mathbf{V}^{(3)} = -\frac{2\mu_0 D_T}{3} \ln \text{Re} \left[\mathbf{V} - \varepsilon_u \left(\mathbf{V} - \frac{3}{4} \mathbf{V}_{\perp} \right) \right] \ln(\bar{T} \bar{P}^{1/7-1}), \quad (29)$$

and for fast rotation, $\Omega_*^2 \gg 1$, the effective pumping velocity $\mathbf{V}^{(3)}$ is given by

$$\mathbf{V}^{(3)} = -\frac{\mu_0 D_T}{2} \left[\ln \text{Re} \mathbf{V}_{\perp} - \left(\frac{\pi \Omega_*}{\varepsilon_u} \right) \hat{\Omega} \times \mathbf{V}_{\perp} \right] \ln(\bar{T} \bar{P}^{1/7-1}), \quad (30)$$

where $\mu_0 = 2V_g L_p / (3D_T)$ with $V_g = \tau_p \mathbf{g}$ being the terminal fall velocity of particles and $L_p = |\nabla \bar{P} / \bar{P}|^{-1}$ being the height scale of the mean pressure. Here, we use the equation of state for the ideal gas, $\bar{P} = R \bar{\rho} \bar{T}$, with $R = k_B / m_{\mu}$ being the gas constant, m_{μ} is the mass of a molecule of the surrounding fluid and k_B is the Boltzmann constant. We also take into account that in the basic reference state for the fluid (i.e., in the hydrostatic equilibrium with a zero mean fluid velocity), $\nabla \bar{P} \approx \bar{\rho} \mathbf{g}$ and $\tau_p k_B / m_{\mu} = V_g L_p / \bar{T}$. The latter expression follows from the identity of the Stokes time for particles $\tau_p = \bar{\rho} V_g L_p / \bar{P}$.

The effective pumping velocity $\mathbf{V}^{(3)}$ is related to the phenomenon of turbulent thermal diffusion for inertial particles. The mechanism of

this effect is as follows. The inertia causes particles inside the turbulent eddies to drift out to the boundary regions between eddies due to the centrifugal inertial force. Indeed, for large Péclet numbers, when molecular diffusion of particles can be neglected in the equation for particle number density, it follows that

$$\nabla \cdot \mathbf{V} \approx -n_p^{-1} \left[\frac{\partial n_p}{\partial t} + (\mathbf{V} \cdot \nabla) n_p \right] \equiv -n_p^{-1} \frac{dn_p}{dt}. \quad (31)$$

On the other hand, for inertial particles, $\nabla \cdot \mathbf{V} = (\tau_p/\rho)\nabla^2 P$. Therefore, in regions with maximum fluid pressure fluctuations (where $\nabla^2 P < 0$), there is an accumulation of inertial particles, i.e., $dn'/dt \propto -\bar{n} (\tau_p/\bar{\rho}) \nabla^2 P > 0$. These regions have low vorticity and high strain rate. Similarly, there is an outflow of inertial particles from regions with minimum fluid pressure.

In homogeneous and isotropic turbulence with a zero gradient of the mean temperature, there is no preferential direction, so that there is no large-scale effect of particle accumulation, and the pressure (temperature) of the surrounding fluid is not correlated with the turbulent velocity field. The only non-zero correlation is $\langle (\mathbf{u} \cdot \nabla) P \rangle$, which contributes to the flux of the turbulent kinetic energy density.

In temperature-stratified turbulence, fluctuations of fluid temperature θ and velocity \mathbf{u} are correlated due to a non-zero turbulent heat flux, $\langle \theta \mathbf{u} \rangle \neq \mathbf{0}$. Fluctuations in temperature cause pressure fluctuations, which result in fluctuations in the number density of particles. Increase of the pressure of the surrounding fluid is accompanied by an accumulation of particles, and the direction of the mean flux of particles coincides with that of the turbulent heat flux. The mean flux of particles is directed toward the minimum of the mean temperature, and the particles tend to accumulate in this region.

To demonstrate that the directions of the mean flux of particles and the turbulent heat flux coincide, we assume that the mean temperature \bar{T}_2 at point 2 is larger than the mean temperature \bar{T}_1 at point 1. We consider two small control volumes “a” and “b” located between these two points. Let the direction of the local turbulent velocity in volume “a” at some instant be the same as the direction of the turbulent heat flux $\langle \theta \mathbf{u} \rangle$ (i.e., along the x -axis toward point 1) and let the local turbulent velocity in volume “b,” at the same instant, be directed opposite to the turbulent heat flux (i.e., toward point 2).

In temperature stratified turbulence with a non-zero turbulent heat flux $\langle \theta \mathbf{u} \rangle$, fluctuations of pressure p and velocity \mathbf{u} are correlated, and regions with a higher level of pressure fluctuations have higher temperature and velocity fluctuations. Fluctuations of temperature θ and pressure P in volume “a” are positive because $\theta u_x > 0$, and negative in volume “b.” Fluctuations of particle number density n' are positive in volume “a” (because particles are locally accumulated in the vicinity of the maximum of pressure fluctuations, $dn'/dt \propto -\bar{n} (\tau_p/\bar{\rho}) \nabla^2 P > 0$), and they are negative in volume “b” (because there is an outflow of particles from regions with low pressure fluctuations). The flux of particles $n' \mathbf{V}$ is positive in volume “a” (i.e., it is directed toward point 1), and it is also positive in volume “b” (because both fluctuations of velocity and number density of particles are negative in volume “b”), where \mathbf{V} is the particle velocity along the x -axis. Therefore, the mean flux of particles $\langle n' \mathbf{V} \rangle$ is directed, as is the turbulent heat flux $\langle \theta \mathbf{u} \rangle$, toward point 1. This causes the formation of large-scale inhomogeneous structures in the spatial distribution of inertial particles in the vicinity of the mean temperature minimum.

The increase in the rotation rate increases the anisotropy of turbulence, and fast rotation results in the effective pumping velocity is in the plane perpendicular to the rotation axis.

D. The effective pumping velocity $V^{(4)}$

Now, we determine the effective pumping velocity $V^{(4)} = -\langle \tau_p/\bar{\rho} \rangle \langle \tau \mathbf{u} (\hat{\Omega} \cdot \nabla)^2 P \rangle$, that is given by Eq. (A17) in Appendix A. For slow rotation, $\Omega_*^2 \ll 1$, the effective pumping velocity $V^{(4)}$ is given by

$$V^{(4)} = -\frac{\mu_0 D_T}{3} \ln \text{Re} \nabla \ln (\bar{T} \bar{P}^{1/\gamma-1}), \quad (32)$$

and for fast rotation, $1 \ll \Omega_*^2 \ll \text{Re}$, the effective pumping velocity $V^{(4)}$ is given by

$$V^{(4)} = -\frac{\mu_0 D_T}{3\varepsilon_u} \left[\ln \left(\frac{\text{Re}}{\Omega_*^2} \right) + \frac{2}{3} \right] \nabla \ln (\bar{T} \bar{P}^{1/\gamma-1}). \quad (33)$$

Since for fast rotation $\Omega_* \gg 1$, the degree of anisotropy ε_u of turbulent velocity field is large ($\varepsilon_u \gg 1$), the effective pumping velocity $V^{(4)}$ vanishes.

E. The effective pumping velocity $V^{(5)}$

Now, we determine the effective pumping velocity $V^{(5)} = -\langle \tau \mathbf{u} (\hat{\Omega} \cdot \text{rot } \mathbf{u}) \rangle$, that is given by Eq. (A18) in Appendix A. For slow rotation, $\Omega_*^2 \ll 1$, the effective pumping velocity $V^{(5)}$ is given by

$$V^{(5)} = -\frac{1}{4} \left[\hat{\Omega} \times \lambda_{\perp} + \frac{3}{2} \hat{\Omega} \times \mathbf{v}_{\perp} - \frac{4}{9} \hat{\Omega} (\hat{\Omega} \cdot \lambda) \right] D_T, \quad (34)$$

and for fast rotation, $\Omega_*^2 \gg 1$, the effective pumping velocity $V^{(5)}$ is given by

$$V^{(5)} = D_T \left[\Omega_* \lambda_{\perp} - \frac{3}{2} \hat{\Omega} \times \lambda_{\perp} \right]. \quad (35)$$

The mechanism for the appearance of an additional mean turbulent flux of particles for fast rotation in the plane perpendicular to the rotation axis is as follows. There are particle containing eddies with the vorticity $\nabla \times \mathbf{u}$ which is parallel (the left-handed eddies) and antiparallel (the right-handed eddies) to the global rotation $\hat{\Omega}$. The fluid density stratification in the plane perpendicular to the rotation axis breaks a symmetry between number of the left-handed and right-handed eddies. This results in the appearance of a non-zero effective pumping velocity $V^{(5)} = -\langle \tau \mathbf{u} (\hat{\Omega} \cdot \text{rot } \mathbf{u}) \rangle$ of particles in the direction of the density stratification.

For fast rotation ($\Omega_*^2 \gg 1$), the total effective pumping velocity is given by

$$\mathbf{V}^{(\text{eff})} = f_1(\omega) D_T \lambda_{\perp} + f_2(\omega) D_T \hat{\Omega} \times \lambda_{\perp}, \quad (36)$$

where

$$f_1(\omega) = 2\Omega_* \omega^3 (1 + 3\omega^2) (1 + \omega^2)^{-4}, \quad (37)$$

$$f_2(\omega) = -4\Omega_* \omega^6 (1 + \omega^2)^{-4}. \quad (38)$$

In Fig. 1, we show the functions $f_1(\omega)$ and $f_2(\omega)$ entering to the total effective pumping velocity (36) for fast rotating turbulence

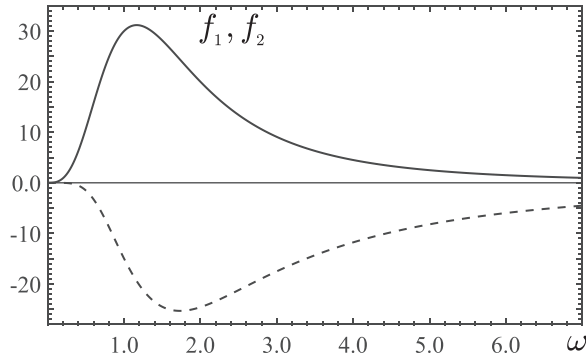


FIG. 1. Functions $f_1(\omega)$ (solid) and $f_2(\omega)$ (dashed) for $\Omega_* = 60$.

($\Omega_* = 60$). In the next section, we analyze the behavior of the total effective pumping velocity (36) for a fast rotating turbulence.

IV. APPLICATIONS TO FORMATION OF PLANETESIMALS IN ACCRETION PROTOPLANETARY DISCS

The analyzed effects are important in astrophysical turbulence, e.g., formation of planetesimals (progenitors of planets) in accretion protoplanetary disks.^{9–14} Small-scale planetesimals are formed from grains and dust in the gaseous protostellar disks or the solar nebula due to coagulation. Inertia of particles advected by turbulent rotating fluid flow causes formation of large-scale inhomogeneities of particles distribution.

The typical parameters of the protosolar nebula are^{9,11,13,14}: the angular velocity $\Omega \sim 2 \times 10^{-7} r_{\text{AU}}^{-3/2} \text{ s}^{-1}$ (where r_{AU} is the radial coordinate measured in the astronomical units $L_{\text{AU}} = 1.5 \times 10^{13} \text{ cm}$); the sound speed $c_s = 6.4 \times 10^4 r_{\text{AU}}^{-3/14} \text{ cm/s}$; the integral scale of turbulence $\ell_0 = \sqrt{\alpha} c_s / \Omega$; the turbulent velocity $u_0 = \alpha c_s$; the turbulent time $\tau_0 = \ell_0 / u_0 = (\sqrt{\alpha} \Omega)^{-1}$; and the turbulent diffusion coefficient $D_T = \ell_0 u_0 / 3$ varies from $2 \times 10^{11} r_{\text{AU}}^{15/14}$ to $10^{13} r_{\text{AU}}^{15/14} \text{ cm}^2/\text{s}$. The kinematic viscosity $\nu = c_s \lambda_{\text{mfp}} / 2 = 1.6 \times 10^5 r_{\text{AU}}^{18/7} \text{ cm}^2/\text{s}$, so the Reynolds number $\text{Re} = \ell_0 u_0 / \nu$ varies from $3 \times 10^6 r_{\text{AU}}^{-3/2}$ to $10^8 r_{\text{AU}}^{-3/2}$. Here, $\lambda_{\text{mfp}} = 5 r_{\text{AU}}^{39/14} \text{ cm}$ is the mean-free path of the gas molecules, α varies from 10^{-3} to 10^{-2} . Therefore, the parameter $\Omega_* = 4\Omega\tau_0 = 4/\sqrt{\alpha}$ varies from 40 to 120. This implies that turbulence in the protosolar nebula is a fast rotating turbulence.

The stopping time τ_p describing particle and fluid interaction depends on the ratio of the mean-free path λ_{mfp} of the gas molecules to the particle radius a_p . In the Epstein regime ($\lambda_{\text{mfp}} > a_p$), the stopping time is $\tau_p = \rho_p a_p / (\bar{\rho} c_s) = 2 \times 10^4 r_{\text{AU}}^{18/7} a_p$, where the particle radius a_p is measured in cm and τ_p is measured in s. Therefore, the parameter $\omega = 2\Omega\tau_p$ is $\omega = 10^{-2} r_{\text{AU}}^{15/14} a_p$. In the Stokes regime ($\lambda_{\text{mfp}} \ll a_p$), the stopping time is $\tau_p = 2\rho_p a_p^2 / (9\bar{\rho} \nu) = 2 \times 10^3 r_{\text{AU}}^{3/14} a_p^2$. Therefore, the parameter $\omega = 10^{-3} r_{\text{AU}}^{-9/7} a_p^2$.

In Fig. 2, we show the radial profiles of the parameter $\omega(r_{\text{AU}})$ for different particle radii: $a_p = 5 \text{ cm}$ (solid), 10 cm (dashed), and 50 cm (dashed-dotted). The decreased function $\omega(r_{\text{AU}})$ corresponds to the Stokes regime, while the increased function $\omega(r_{\text{AU}})$ corresponds to the

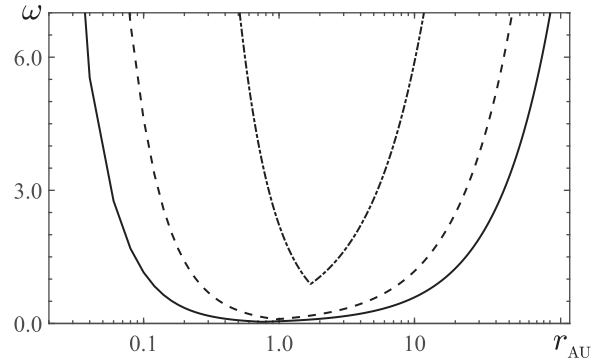


FIG. 2. Radial profiles of the parameter $\omega(r_{\text{AU}})$ for different particle radii: $a_p = 5 \text{ cm}$ (solid), 10 cm (dashed), and 50 cm (dashed-dotted). Here, r_{AU} is the radial coordinate measured in the astronomical units $L_{\text{AU}} = 1.5 \times 10^{13} \text{ cm}$.

Epstein regime. To plot Fig. 2, we use Eq. (1) from¹⁴ for τ_p with the smooth transition between the Stokes and the Epstein regimes. In particular, the case $a_p \leq 9\lambda_{\text{mfp}}/4$ corresponds to the Epstein regime, while for $a_p > 9\lambda_{\text{mfp}}/4$ the Stokes regime describes τ_p , where $\lambda_{\text{mfp}} = 5 r_{\text{AU}}^{39/14} \text{ cm}$.

The mean fluid density is $\bar{\rho} = 2 \times 10^{-9} r_{\text{AU}}^{-11/4} \text{ g/cm}^3$, the mean fluid temperature is $\bar{T} = 280 r_{\text{AU}}^{-1/2} \text{ K}$, the parameter $\mu_0 D_T = (2/3\gamma) \tau_p c_s^2$, the scale $H_g = c_s / \Omega = 3 \times 10^{11} r_{\text{AU}}^{9/7} \text{ cm}$. Note that in the radial direction, the gravity force acting on the particles is compensated by the centrifugal force. This is the reason why these forces are not included in Eqs. (5) and (6). In Fig. 3, we plot the radial profiles of the azimuthal $V_\phi^{(\text{eff})}(r_{\text{AU}})$ and radial $V_r^{(\text{eff})}(r_{\text{AU}})$ components of the total effective velocity for different particle radii a_p from 5 to 50 cm for fast rotating turbulence ($\Omega_* = 60$). The effective pumping velocity components for fast rotating turbulence are determined by Eq. (36), where λ_\perp is directed in the radial direction. These radial profiles have two maxima corresponding to different regimes of the particle–fluid interactions: at the small radius it is the Stokes regime, while at the larger radius it is the Epstein regime. With the decrease in the particle radius, the distance between the

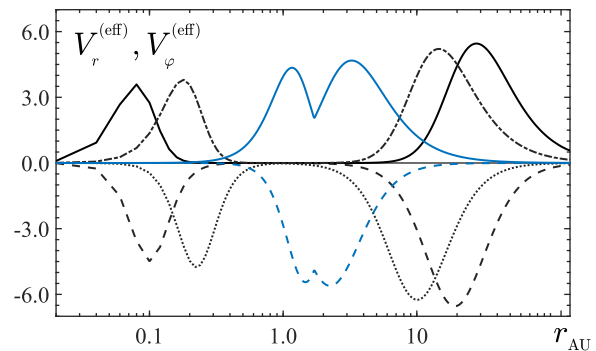


FIG. 3. Radial profiles of the azimuthal $V_\phi^{(\text{eff})}(r_{\text{AU}})$ component of the effective velocity for different particle radii: $a_p = 5 \text{ cm}$ (solid), 10 cm (dashed-dotted), and 50 cm (solid blue); and of the radial component $V_r^{(\text{eff})}(r_{\text{AU}})$ of the effective velocity for different particle sizes $a_p = 5 \text{ cm}$ (dashed), 10 cm (dotted), 50 cm (dashed blue) for $\Omega_* = 60$ (that corresponds to $\alpha = 1/225$). The velocity is measured in cm/s.

maxima increases. This implies that smaller-size particles are concentrated near the central body of the accretion disk, while larger-size particles are accumulated far from the central body.

In Fig. 4, we plot the equilibrium radial profile of the mean particle number density $\bar{n}(r_{\text{AU}})$ for different particle radii a_p from 5 to 50 cm for fast rotating turbulence ($\Omega_* = 60$). The equilibrium radial profile of the mean particle number density $\bar{n}(r_{\text{AU}})$ is determined by the steady-state solution of Eq. (2)

$$\bar{n}(r_{\text{AU}}) = \bar{n}_* \exp\left(-\int_{r_{\text{min}}}^{r_{\text{AU}}} \frac{V_r^{\text{(eff)}}(r')}{D_T(r')} dr'\right). \quad (39)$$

It follows from Fig. 4 that the size of particle cluster increases with the particle radius. Note that the material density of particles ρ_p as well as their radius a_p affect the particle stopping time. With increase in ρ_p and a_p the particle stopping time increases. The characteristic formation time of large-scale particle clusters is about $\tau_{\text{dyn}} = r/V_r^{\text{(eff)}} \sim 10^5\text{--}10^6$ years, where $r_{\text{AU}} = 1\text{--}10$ (measured in the astronomical units L_{AU}) and $V_r^{\text{(eff)}} \sim 5$ cm/s. Note that the turbulent diffusion time is about $\tau_{\text{diff}} = r^2/D_T \sim (0.4\text{--}3) \times 10^7$ years. The turbulent diffusion affects the lifetime of the large-scale clusters, and τ_{diff} is much larger than the characteristic formation time of large-scale particle cluster ($\sim \tau_{\text{dyn}}$).

V. DISCUSSION AND CONCLUSIONS

A theory of large-scale clustering of inertial particles (in scales which are much larger than the turbulent integral scale) in a rotating density stratified or inhomogeneous turbulence is developed. The large-scale particle clustering is characterized by the effective pumping velocity in a turbulent flux of particles, which for a fast rotation is localized in the plane perpendicular to rotation axis along the fluid density stratification. This causes the formation of large-scale inhomogeneities in particle spatial distribution. The developed theory of the large-scale particle clustering has been applied for explanation of the formation of planetesimals (progenitors of planets) in accretion protoplanetary disks.

We apply mean-field theory to describe large-scale clustering phenomena in rotating and stratified turbulence. The mean-field theory is valid when the characteristic spatial (and/or temporal) scales of the mean-field variations are much larger than the integral turbulence

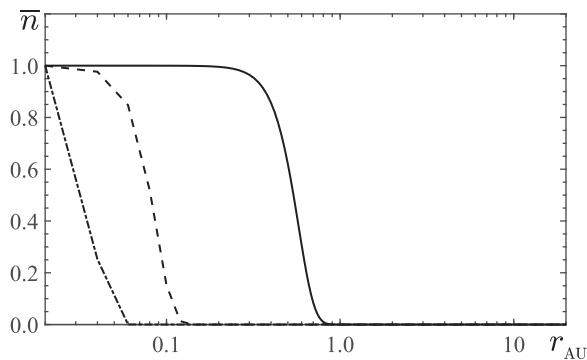


FIG. 4. Equilibrium radial profile of the normalized mean particle number density $\bar{n}(r_{\text{AU}})$ for different particle radii: $a_p = 5$ cm (dashed-dotted), 10 cm (dashed), and 50 cm (solid); and for $\Omega_* = 60$.

scale (and/or turbulence correlation time). The applicability of a mean-field theory in fast rotating and stratified turbulence based on the τ approach has been discussed in Ref. 40, where comparison with results of direct numerical simulations (see Refs. 45 and 46) has been performed. In these papers, a generation of a large-scale vorticity in a fast rotating density stratified turbulent convection has been studied.

The theory⁴⁰ predicts the threshold in the Coriolis number requires for the generation of the large-scale vorticity observed in DNS.^{45,46} The critical Coriolis number should be much larger than 1. The derived mean-field equations describe formations of both, cyclonic and anticyclonic large-scale vortices in the kinematic (linear) stage of the instability. As in the DNS, the theory⁴⁰ predicts the similar behavior of the mean entropy or temperature inside cyclonic and anticyclonic vortices: for the mode with the dominant vertical mean vorticity, the mean entropy is decreased inside the cyclonic vortices and increased inside the anticyclonic vortices in agreement with DNS. Detailed validation of the developed mean-field theory of large-scale clustering in rotating density-stratified turbulence in numerical simulations is a subject of future separate studies.

To derive equations for the rotational contribution to the Reynolds stress and the turbulent heat flux in rotating density stratified turbulence, we apply the spectral τ approach (see Sec. II and Appendix B). The τ approach is valid for large fluid and magnetic Reynolds numbers and for large Péclet numbers. In this case, turbulence is strong, and the relaxation time τ_r in Eq. (B8) can be identified with the scale-dependent turbulent time $\tau(k)$ (see the Appendix B). However, the τ approach does not work to study intermittency of scalar and magnetic fluctuations.

The τ approach reproduces many well-known phenomena found by other methods in turbulent transport of particles, temperature and magnetic fields, in turbulent convection and stably stratified turbulent flows (see detailed discussion in Ref. 8, and references therein). In particular, in turbulent transport of particles, the τ approximation yields correct formulas for turbulent diffusion, turbulent thermal diffusion, and turbulent barodiffusion obtained by other methods. The phenomenon of turbulent thermal diffusion (a nondiffusive streaming of particles in the direction of the turbulent heat flux), has been studied using the stochastic calculus (the path integral approach), the quasi-linear approach, the direct interaction approximation (DIA) and the τ approach (see Ref. 8, and references therein). The phenomenon of turbulent thermal diffusion and large-scale particle clustering has been already detected in laboratory experiments in non-rotating stably and unstably temperature stratified turbulence,^{31–35} and in direct numerical simulations (DNS) in non-rotating density-stratified turbulence.^{28–30} The numerical and experimental results are in good agreement with the theoretical studies performed by means of different approaches, including the τ approach.

The detailed verification of the τ approach in DNS of turbulent transport of passive scalar has been performed in.⁴⁷ In particular, the results on turbulent transport of passive scalar obtained using DNS have been compared with that obtained using a closure model based on the τ approach. The numerical and analytical results are in a good agreement.

The τ approach reproduces the well-known $k^{-7/3}$ -spectrum of anisotropic velocity fluctuations in a sheared turbulence.^{48,49} This spectrum was previously found in analytical,⁵⁰ numerical,⁵¹ and laboratory studies⁵² and was observed in the atmospheric turbulence.⁵³ In

the turbulent boundary layer problems, the τ approach yields correct expressions for turbulent viscosity, turbulent thermal conductivity, and the classical turbulent heat flux. This approach also describes the counter-wind heat flux and the Deardorff's heat flux in convective turbulence.^{48,49} These phenomena have been previously studied using different analytical approaches (see Ref. 8, and references therein).

In magnetohydrodynamics, the τ approach reproduces many well-known phenomena found by different methods, e.g., the τ approach yields correct formulas for the α -effect, the effective pumping velocities, and the turbulent magnetic diffusion in rotating and density stratified turbulence (see Ref. 8, and references therein). These results also have been confirmed using DNS in forced turbulence as well as in rotating density-stratified turbulence.^{29,54} In high-energy physics, e.g., in chiral magnetohydrodynamics, DNS reproduces many results predicted using the τ approach.^{55–59}

Comparisons of theoretical predictions and DNS performed for various turbulence problems (where large-scale effects are caused by turbulence) show that often the separation of scales characterized by the ratio of typical scale of mean-field variations to the integral scale of turbulence should be in DNS in the interval from 3 to 5. This allows us to observe in DNS the large-scale effects caused by turbulence. However, there is a case when the scale separation ratio should be much larger. For instance, the negative effective magnetic pressure instability (NEMPI),^{60,61} which results in the formation of the large-scale magnetic flux tubes, requires the scale separation ratio in the interval from 15 to 30. This allows us to observe this instability in DNS.^{60,61}

In the present study, we consider large-scale clustering in a low-Mach-number turbulence. These conditions are relevant for applications to the formation of planetesimals in accretion protoplanetary disks. The weak correlation between fluid density and velocity fluctuations at low-Mach-number turbulence is discussed in Ref. 62. The effects of compressibility (not small Mach numbers) on the turbulent diffusivity and the effective pumping velocity of particles for non-rotating density stratified or inhomogeneous turbulence are discussed in Sec. 2.5 in Ref. 8, see references therein. The theoretical predictions of the compressibility effects on turbulent transport of particles are in agreement with DNS results for non-rotating density stratified or inhomogeneous turbulence.^{29,30} The effects of compressibility on the large-scale particle clustering in a rotating density stratified and inhomogeneous turbulence is the subject of future separate studies.

In the developed theory of large-scale particle clustering, the stopping time τ_p which describes the fluid-particle interaction regimes, enters only in the parameter $\omega = 2\Omega\tau_p$, and the theory is developed for arbitrary parameter ω . In the applications of the analyzed effects for an explanation of the formation of planetesimals in protoplanetary disks, we consider two different fluid-particle interaction regimes. In particular, the stopping time τ_p depends on the ratio of the mean-free path λ_{mfp} of the gas molecules to the particle radius a_p . When $\lambda_{\text{mfp}}/a_p > 1$, the Epstein regime of the fluid-particle interaction describes τ_p , while for $\lambda_{\text{mfp}}/a_p \ll 1$, the Stokes regime describes τ_p . When the ratio $\lambda_{\text{mfp}}/a_p < 1$, and it is not small, there is a smooth transition between these regimes. For instance, to plot Fig. 2 for the radial profiles of the parameter $\omega(r_{\text{AU}})$, we use Eq. (1) from Ref. 14 for τ_p with the smooth transition between the Stokes and the Epstein

regimes (see Sec. IV). Another way is to use Eq. (10) from Ref. 63 for τ_p with the smooth transition between different regimes. However, this only affects the parameter ω .

In this paper we analyze the reasons for large-scale clustering caused by the turbulent effects, which are described in terms of the effective pumping velocity in the mean-field equation for the mean particle number density. The derived pumping velocities are independent of boundary conditions. These pumping velocities arise due to small-scale turbulence in the presence of rotation and stratification.

To determine the characteristics of the large-scale clusters, like dimensions (the characteristic length and width) and shape (aspect ratio) of the large-scale clusters, and time evolution of clusters, one needs to solve the derived nonlinear mean-field equations which include the derived effective pumping velocities. This can be done by the mean-field numerical simulations (MFS) which is the subject of future separate comprehensive studies. The subsequent particle distributions in the clusters obtained in MFS may depend on boundary conditions. Note also that a mean-field theory is able to take into account the back-reactions of particles on turbulence which are important when the mass-loading parameter $m_p \bar{n} / \bar{\rho}$ inside the cluster is of the order of or larger than 1. These nonlinear effects can be studied in MFS.

In the developed theory there are two key parameters: $\omega = 2\tau_p\Omega$ and $\Omega_* = 4\Omega\tau_0$. The stopping time of particles $\tau_p \ll \tau_0$ is the smallest time in the system, and the theory is valid for large Reynolds numbers and for large Péclet numbers. The developed theory can be also applied to large-scale clustering of dust in accretion disks in binary stellar system and in young galactic rotating accretion disks.

ACKNOWLEDGMENTS

I.R. would like to thank the Isaac Newton Institute for Mathematical Sciences, Cambridge, for support and hospitality during the program “Anti-diffusive dynamics: from sub-cellular to astrophysical scales,” where this work was initiated. I.R. acknowledges the discussions with some participants of the Nordita Scientific Program on “Stellar convection: modelling, theory and observations,” Stockholm (September 2024), which is partly supported by NordForsk.

AUTHOR DECLARATIONS

Conflict of Interest

The authors have no conflicts to disclose.

Author Contributions

Nathan Kleorin: Conceptualization (equal); Formal analysis (equal); Investigation (equal); Methodology (equal); Validation (equal); Writing – original draft (equal). **Igor Rogachevskii:** Conceptualization (equal); Formal analysis (equal); Investigation (equal); Methodology (equal); Validation (equal); Writing – original draft (equal).

DATA AVAILABILITY

The data that support the findings of this study are available from the corresponding author upon reasonable request.

APPENDIX A: TOTAL EFFECTIVE PUMPING VELOCITY OF PARTICLES

In this appendix, we derive the total effective pumping velocity $\mathbf{V}^{(\text{eff})} = -\langle \tau \mathbf{V} \text{div} \mathbf{V} \rangle$ for arbitrary values of parameter ω . To determine $\text{div} \mathbf{V}$ [given by Eq. (10)], we assume that the parameter ω and the Stokes time τ_p are independent parameters. Using Eq. (9), we find $d\mathbf{V}/dt$ for small Stokes time applying a method of iterations. This yields

$$-\tau_p \frac{d\mathbf{V}}{dt} = \frac{\omega}{1 + \omega^2} \left[\hat{\Omega} \times \mathbf{u} + \omega (\mathbf{u} - \hat{\Omega} (\hat{\Omega} \cdot \mathbf{u})) + \frac{\tau_p}{\rho} (\omega^{-1} \nabla + \omega \hat{\Omega} (\hat{\Omega} \cdot \nabla) - \hat{\Omega} \times \nabla) P \right] + O(\tau_p^2), \quad (\text{A1})$$

and

$$-\tau_p B_{mi} \frac{dV_i}{dt} = \frac{\omega^2}{1 + \omega^2} \left[\mathbf{u} - \omega \hat{\Omega} \times \mathbf{u} - \hat{\Omega} (\hat{\Omega} \cdot \mathbf{u}) - \frac{\tau_p}{\rho} (\nabla - (2 + \omega^2) \hat{\Omega} (\hat{\Omega} \cdot \nabla) + \omega^{-1} \hat{\Omega} \times \nabla) P \right] + O(\tau_p^2), \quad (\text{A2})$$

where $\hat{\Omega} = \mathbf{\Omega}/\Omega$ is the unit vector and we use Eq. (6) for large Reynolds numbers (which allows us to neglect small term proportional to the kinematic viscosity). Equations (10) and (A1)–(A2) allow us to find the compressibility of particle velocity field characterized by $\text{div} \mathbf{V}$

$$\begin{aligned} \text{div} \mathbf{V} &= \text{div} \mathbf{u} + \frac{\tau_p}{\rho} (\Delta + \boldsymbol{\lambda} \cdot \nabla) P + \frac{\omega^2}{(1 + \omega^2)^2} \\ &\times \left\{ 2\omega \hat{\Omega} \cdot \text{rot} \mathbf{u} + (1 - \omega^2) \text{div} \mathbf{u}_\perp - \frac{\tau_p}{\rho} \left[(3 + \omega^2) \right. \right. \\ &\left. \left. \times (\Delta_\perp + \boldsymbol{\lambda}_\perp \cdot \nabla) + 2\omega^{-1} (\hat{\Omega} \times \boldsymbol{\lambda}_\perp) \cdot \nabla \right] P \right\} + O(\tau_p^2), \end{aligned} \quad (\text{A3})$$

where $\boldsymbol{\lambda} = -\bar{\rho}^{-1} \nabla \bar{\rho}$. For the derivation of Eqs. (A1)–(A3), we used the following identities: $B_{mi} \nabla_i = \omega^2 [\hat{\Omega} (\hat{\Omega} \cdot \nabla) - \omega^{-1} \hat{\Omega} \times \nabla]_m$

$$-\tau_p \text{div} \left(\frac{d\mathbf{V}}{dt} \right) = \frac{1}{1 + \omega^2} (\delta_{mi} + B_{mi}) \left[\frac{\tau_p}{\rho} (\nabla_m + \lambda_m) \nabla_i P - \omega \varepsilon_{ipq} \hat{\Omega}_q \nabla_m u_p \right] + O(\tau_p^2), \quad (\text{A4})$$

$$B_{mi} \nabla_i \nabla_m P = \omega^2 (\hat{\Omega} \cdot \nabla)^2 P, \quad (\text{A5})$$

$$B_{mi} (\nabla_i P) \lambda_m = \omega \left[\hat{\Omega} \cdot (\boldsymbol{\lambda}_\perp \times \nabla) + \omega (\hat{\Omega} \cdot \boldsymbol{\lambda}) (\hat{\Omega} \cdot \nabla) \right] P, \quad (\text{A6})$$

$$B_{mi} \varepsilon_{ipq} \hat{\Omega}_q u_p = \omega [\hat{\Omega}_m (\hat{\Omega} \cdot \mathbf{u}) - u_m], \quad (\text{A7})$$

$$B_{mi} \varepsilon_{ipq} \hat{\Omega}_q \nabla_m u_p = -\omega \text{div} \mathbf{u}_\perp. \quad (\text{A8})$$

This yields also

$$-\tau_p \text{div} \left(\frac{d\mathbf{V}}{dt} \right) = \frac{\tau_p}{\rho} \left[\Delta + \boldsymbol{\lambda} \cdot \nabla - \frac{\omega^2}{1 + \omega^2} (\Delta_\perp + \boldsymbol{\lambda}_\perp \cdot \nabla - \omega^{-1} \hat{\Omega} \cdot (\boldsymbol{\lambda}_\perp \times \nabla)) P - \text{div} \mathbf{u}_\perp + \omega^{-1} \hat{\Omega} \cdot \text{rot} \mathbf{u} \right] + O(\tau_p^2), \quad (\text{A9})$$

and

$$-\tau_p \nabla_m \left(B_{mi} \frac{dV_i}{dt} \right) = \frac{\omega^2}{1 + \omega^2} \left\{ \frac{\tau_p}{\rho} \left[(1 + \omega^2) (\Delta + \boldsymbol{\lambda} \cdot \nabla) - (2 + \omega^2) (\Delta_\perp + \boldsymbol{\lambda}_\perp \cdot \nabla) + \omega^{-1} (\hat{\Omega} \times \boldsymbol{\lambda}) \cdot \nabla \right] P + \text{div} \mathbf{u}_\perp + \omega \hat{\Omega} \cdot \text{rot} \mathbf{u} \right\} + O(\tau_p^2). \quad (\text{A10})$$

Equations (9) and (A1)–(A2) yield the particle velocity field

$$\begin{aligned} \mathbf{V} &= \frac{1}{(1 + \omega^2)^2} \left\{ (1 + 3\omega^2) \mathbf{u} - 2\omega^3 (\hat{\Omega} \times \mathbf{u}) \right. \\ &\left. - (1 - \omega^2) \omega^2 (\hat{\Omega} \cdot \mathbf{u}) \hat{\Omega} + \frac{\tau_p}{\rho} \left[(1 - \omega^2) \nabla \right. \right. \\ &\left. \left. + (3 + \omega^2) \omega^2 \hat{\Omega} (\hat{\Omega} \cdot \nabla) - 2\omega (\hat{\Omega} \times \nabla) \right] P \right\}. \end{aligned} \quad (\text{A11})$$

Equations (A3) and (A11) for $\omega^2 \ll 1$ read

$$\begin{aligned} \text{div} \mathbf{V} &= (1 + \omega^2) \text{div} \mathbf{u} - \omega^2 (\hat{\Omega} \cdot \nabla) (\hat{\Omega} \cdot \mathbf{u}) \\ &+ \frac{\tau_p}{\rho} \left[(1 - 3\omega^2) (\Delta + \boldsymbol{\lambda} \cdot \nabla) + 3\omega^2 \left[(\hat{\Omega} \cdot \nabla)^2 \right. \right. \\ &\left. \left. + (\hat{\Omega} \times \boldsymbol{\lambda}) (\hat{\Omega} \cdot \nabla) \right] + 2\omega (\hat{\Omega} \times \boldsymbol{\lambda}_\perp) \cdot \nabla \right] P + O(\tau_p^2), \end{aligned} \quad (\text{A12})$$

and

$$\begin{aligned} \mathbf{V} &= (1 + \omega^2) \mathbf{u} - \omega^2 \hat{\Omega} (\hat{\Omega} \cdot \mathbf{u}) + \frac{\tau_p}{\rho} \left[(1 - 3\omega^2) \nabla \right. \\ &\left. + 3\omega^2 \hat{\Omega} (\hat{\Omega} \cdot \nabla) - 2\omega (\hat{\Omega} \times \nabla) \right] P + O(\tau_p^2). \end{aligned} \quad (\text{A13})$$

By means of Eqs. (A3) and (A11), we determine the total effective pumping velocity: $\mathbf{V}^{(\text{eff})} = -\langle \tau \mathbf{V} \text{div} \mathbf{V} \rangle$, which is given by Eq. (11), where the effective pumping velocity $\mathbf{V}^{(1)} = -\langle \tau \mathbf{u} \text{div} \mathbf{u} \rangle$ is

$$\begin{aligned} \mathbf{V}^{(1)} &= -\frac{1}{1 + \varepsilon_u} \left\{ 2A_1^{(1)}(\Omega_*) \boldsymbol{\lambda} + \left[A_2^{(1)}(\Omega_*) + \frac{3}{4} \varepsilon_u \right] \boldsymbol{\lambda}_\perp \right. \\ &\left. - \Omega_* A_3^{(2)}(\Omega_*) \left[\hat{\Omega} \times \left(\boldsymbol{\lambda}_\perp - \frac{1}{2} \mathbf{V}_\perp \right) \right] \right\} D_T. \end{aligned} \quad (\text{A14})$$

The functions $A_n^{(m)}(\Omega_*)$ are given in Appendix C. The effective pumping velocity $\mathbf{V}^{(2)} = -\langle \tau \mathbf{u} (\hat{\Omega} \cdot \nabla) (\hat{\Omega} \cdot \mathbf{u}) \rangle$ is given by

$$\begin{aligned} \mathbf{V}^{(2)} &= \frac{1}{2(1 + \varepsilon_u)} \left[(A_1^{(1)}(\Omega_*) - A_2^{(1)}(\Omega_*)) \hat{\Omega} (\hat{\Omega} \cdot \nabla) \right. \\ &\left. + 2A_3^{(1)}(\Omega_*) \boldsymbol{\lambda}_\perp + 2\Omega_* \left(A_2^{(2)}(\Omega_*) + \frac{4}{5} C_1^{(2)}(\Omega_*) \right) \right. \\ &\left. \times \left[\hat{\Omega} \times \left(\boldsymbol{\lambda}_\perp - \frac{1}{2} \mathbf{V}_\perp \right) \right] \right] D_T. \end{aligned} \quad (\text{A15})$$

The functions $A_n^{(m)}(\Omega_*)$ and $C_n^{(m)}(\Omega_*)$ are given in Appendix C. The effective pumping velocity $\mathbf{V}^{(3)} = -\langle \tau_p / \bar{\rho} \rangle \langle \tau \mathbf{u} \Delta P \rangle$ is given by

$$\begin{aligned} \mathbf{V}^{(3)} = & -\frac{2\mu_0 D_T}{3(1+\varepsilon_u)} \left\{ 2A_1^{(-1)}(\Omega_*) \mathbf{V} + \left[A_2^{(-1)}(\Omega_*) \right. \right. \\ & \left. \left. + \frac{3\varepsilon_u}{4} \ln \operatorname{Re} \right] \mathbf{V}_\perp - \Omega_* A_3^{(0)}(\Omega_*) \hat{\Omega} \times \mathbf{V}_\perp \right\} \\ & \times \ln(\bar{T} \bar{P}^{1/\gamma-1}). \end{aligned} \quad (\text{A16})$$

The effective pumping velocity $\mathbf{V}^{(4)} = -(\tau_p/\bar{\rho}) \langle \tau \mathbf{u} (\hat{\Omega} \cdot \mathbf{V})^2 P \rangle$ is given by

$$\begin{aligned} \mathbf{V}^{(4)} = & -\frac{2\mu_0 D_T}{15(1+\varepsilon_u)} \left[(5A_3^{(-1)}(\Omega_*) - C_4^{(0)}(\Omega_*)) \mathbf{V} \right. \\ & + (A_2^{(0)}(\Omega_*) - 2A_1^{(0)}(\Omega_*) + 12C_1^{(0)}(\Omega_*)) \hat{\Omega} (\hat{\Omega} \cdot \mathbf{V}) \\ & \left. - \frac{\Omega_*}{2} (A_2^{(0)}(\Omega_*) - A_1^{(0)}(\Omega_*) + 8C_1^{(0)}(\Omega_*)) \hat{\Omega} \times \mathbf{V}_\perp \right] \\ & \times \ln(\bar{T} \bar{P}^{1/\gamma-1}). \end{aligned} \quad (\text{A17})$$

The effective pumping velocity $\mathbf{V}^{(5)} = -\langle \tau \mathbf{u} (\hat{\Omega} \cdot \operatorname{rot} \mathbf{u}) \rangle$ is given by

$$\begin{aligned} \mathbf{V}^{(5)} = & -\frac{\Omega_*}{3(1+\varepsilon_u)} \left\{ (\hat{\Omega} \times \boldsymbol{\lambda}_\perp) \left[\Omega_*^{-1} \left(\frac{9}{2} \varepsilon_u + A_3^{(1)}(\Omega_*) \right) \right. \right. \\ & \left. \left. - 2\Omega_* (A_2^{(3)}(2\Omega_*) + 4C_1^{(3)}(2\Omega_*) - C_4^{(3)}(2\Omega_*)) \right] - 3\varepsilon_u \boldsymbol{\lambda}_\perp \right. \\ & \left. + \boldsymbol{\lambda} \left[\frac{1}{6} - A_1^{(2)}(2\Omega_*) + \frac{43}{5} C_4^{(2)}(\Omega_*) - 4C_4^{(2)}(2\Omega_*) \right] \right. \\ & \left. + \hat{\Omega} (\hat{\Omega} \cdot \boldsymbol{\lambda}) \left[5 - \Omega_*^{-1} A_1^{(2)}(2\Omega_*) + \frac{1}{2} (3A_3^{(2)}(2\Omega_*)) \right. \right. \\ & \left. \left. - 8C_1^{(2)}(2\Omega_*) + 13C_4^{(2)}(2\Omega_*) - \frac{54}{5} C_4^{(2)}(\Omega_*) \right] \right. \\ & \left. + \left[\frac{1}{4} + \frac{37}{10} C_4^{(2)}(\Omega_*) - 2C_4^{(2)}(2\Omega_*) \right] \mathbf{V} + 3 \left[1 + \frac{1}{4} (A_3^{(2)}(2\Omega_*)) \right. \right. \\ & \left. \left. + 3C_4^{(2)}(2\Omega_*) - \frac{6}{5} C_4^{(2)}(\Omega_*) \right] \hat{\Omega} (\hat{\Omega} \cdot \mathbf{V}) \right. \\ & \left. + \frac{1}{2} \Omega_*^{-1} \left[3 - A_3^{(1)}(\Omega_*) \right] \hat{\Omega} \times \mathbf{V}_\perp \right\} D_T. \end{aligned} \quad (\text{A18})$$

For $\omega^2 \ll 1$, the total effective pumping velocity is given by

$$\begin{aligned} \mathbf{V}^{(\text{eff})} = & (1 + 2\omega^2) \mathbf{V}^{(1)} + (1 - 2\omega^2) \mathbf{V}^{(3)} \\ & - \omega^2 \left[\mathbf{V}^{(2)} - 3\mathbf{V}^{(4)} + \hat{\Omega} \left[\hat{\Omega} \cdot (\mathbf{V}^{(1)} + \mathbf{V}^{(3)}) \right] \right]. \end{aligned} \quad (\text{A19})$$

APPENDIX B: EFFECT OF ROTATION ON TURBULENCE

In this appendix, we derive equation for the rotational contributions to the Reynolds stress and turbulent heat flux. We apply the approach developed in Refs. 39 and 40. Equations for fluctuations of velocity \mathbf{u}' and temperature θ' are rewritten in the \mathbf{k} space using new variables for fluctuations of velocity $\mathbf{U} = \sqrt{\bar{\rho}} \mathbf{u}'$ and entropy $s = \sqrt{\bar{\rho}} s'$. Using these equations we derive equations for the following correlation functions: $f_{ij}(\mathbf{k}, \mathbf{K}) = \langle U_i(t, \mathbf{k}_1) U_j(t, \mathbf{k}_2) \rangle$, $F_i(\mathbf{k}, \mathbf{K}) = \langle s(t, \mathbf{k}_1) U_i(t, \mathbf{k}_2) \rangle$, and $\Theta_i(\mathbf{k}, \mathbf{K}) = \langle s(t, \mathbf{k}_1) s(t, \mathbf{k}_2) \rangle$. We apply the multi-scale approach,⁴¹ where $\mathbf{k}_1 = \mathbf{k} + \mathbf{K}/2$,

$\mathbf{k}_2 = -\mathbf{k} + \mathbf{K}/2$, the wave vector \mathbf{K} and the vector $\mathbf{R} = (\mathbf{x} + \mathbf{y})/2$ correspond to the large-scale variables, while \mathbf{k} and $\mathbf{r} = \mathbf{y} - \mathbf{x}$ correspond to the small-scale variables. Hereafter, we omit argument t in the correlation functions. The equations for these correlation functions are given by

$$\frac{\partial f_{ij}(\mathbf{k}, \mathbf{K})}{\partial t} = L_{ijmn}^\Omega f_{mn} + M_{ij}^F + \hat{\mathcal{N}} \tilde{f}_{ij}, \quad (\text{B1})$$

$$\frac{\partial F_i(\mathbf{k}, \mathbf{K})}{\partial t} = D_{im}^\Omega F_m + g_{em} P_{im}(\mathbf{k}_1) \Theta + \hat{\mathcal{N}} \tilde{F}_i, \quad (\text{B2})$$

$$\frac{\partial \Theta(\mathbf{k}, \mathbf{K})}{\partial t} = \hat{\mathcal{N}} \Theta, \quad (\text{B3})$$

where $D_{ij}^\Omega(\mathbf{k}) = 2\varepsilon_{ijm} \Omega_n k_{mn}$, $L_{ijmn}^\Omega = D_{im}^\Omega(\mathbf{k}_1) \delta_{jn} + D_{jn}^\Omega(\mathbf{k}_2) \delta_{im}$, δ_{ij} is the Kronecker unit tensor, $k_{ij} = k_i k_j / k^2$, ε_{ijk} is the Levi-Civita fully antisymmetric tensor, $P_{ij}(\mathbf{k}) = \delta_{ij} - k_{ij}$, and

$$M_{ij}^F = g_{em} [P_{im}(\mathbf{k}_1) F_j(\mathbf{k}, \mathbf{K}) + P_{jm}(\mathbf{k}_2) F_i(-\mathbf{k}, \mathbf{K})]. \quad (\text{B4})$$

In Eqs. (B1)–(B3), $\hat{\mathcal{N}} \tilde{f}_{ij}$ and $\hat{\mathcal{N}} \tilde{F}_i$ are the third-order moments appearing due to the nonlinear terms U_m^N and s^N , which are given by

$$\hat{\mathcal{N}} \tilde{f}_{ij} = \langle P_{im}(\mathbf{k}_1) U_m^N(\mathbf{k}_1) U_j(\mathbf{k}_2) \rangle + \langle U_i(\mathbf{k}_1) P_{jm}(\mathbf{k}_2) U_m^N(\mathbf{k}_2) \rangle, \quad (\text{B5})$$

$$\hat{\mathcal{N}} \tilde{F}_i = \langle s^N(\mathbf{k}_1) U_j(\mathbf{k}_2) \rangle + \langle s(\mathbf{k}_1) P_{im}(\mathbf{k}_2) U_m^N(\mathbf{k}_2) \rangle, \quad (\text{B6})$$

$$\hat{\mathcal{N}} \Theta = \langle s^N(\mathbf{k}_1) s(\mathbf{k}_2) \rangle + \langle s(\mathbf{k}_1) s^N(\mathbf{k}_2) \rangle. \quad (\text{B7})$$

The derived equations for the second-order moments of the velocity fluctuations $\langle U_i U_j \rangle$, the entropy fluctuations $\langle s^2 \rangle$ and the turbulent flux of entropy $\langle s U_i \rangle$, include the first-order spatial differential operators $\hat{\mathcal{N}}$ applied to the third-order moments $M^{(III)}$. A problem arises how to close the system of the second-moment equations, i.e., how to express the set of the third-moment terms $\hat{\mathcal{N}} M^{(III)}(\mathbf{k})$ through the lower moments (see, e.g., Refs. 8 and 42). In the present study, we use the spectral τ approximation (see, e.g., Refs. 8 and 42–44), which postulates that the deviations of the third-moment terms, $\hat{\mathcal{N}} M^{(III)}(\mathbf{k})$, from the contributions to these terms afforded by the background rotating turbulence, $\hat{\mathcal{N}} M^{(III,0)}(\mathbf{k})$, are expressed through the similar deviations of the second-order moments, $M^{(II)}(\mathbf{k}) - M^{(II,0)}(\mathbf{k})$ in the relaxation form

$$\hat{\mathcal{N}} M^{(III)}(\mathbf{k}) - \hat{\mathcal{N}} M^{(III,0)}(\mathbf{k}) = -\frac{M^{(II)}(\mathbf{k}) - M^{(II,0)}(\mathbf{k})}{\tau_r(k)}. \quad (\text{B8})$$

Here, the correlation functions with the superscript (0) correspond to the background non-rotating turbulence. The time $\tau_r(k)$ is the characteristic relaxation time of the statistical moments, which can be identified with the correlation time $\tau(k)$ of the turbulent velocity field for large Reynolds numbers.

The rotational contributions to the Reynolds stress $f_{ij}^{(\Omega)} \equiv \langle U_i(\mathbf{k}_1) U_j(\mathbf{k}_2) \rangle$ and turbulent heat flux $F_i^{(\Omega)} \equiv \langle s(\mathbf{k}_1) U_i(\mathbf{k}_2) \rangle$ follows from Eqs. (B1)–(B8). We also take into account that the characteristic time of variations of the second moments are much larger than the correlation time $\tau(k)$ of the turbulent velocity field. Therefore, the rotational contributions to the Reynolds stress and turbulent heat flux are given by^{39,40,64}

$$f_{ij}^{(\Omega)}(\mathbf{k}) = L_{ijmn}^{-1} \left[f_{mn}^{(0)}(\mathbf{k}) + \tau (L_{mnpq}^\nabla + L_{mnpq}^\perp + \tilde{M}_{mn}^F) f_{pq}^{(0)}(\mathbf{k}) \right], \quad (\text{B9})$$

$$F_i^{(\Omega)}(\mathbf{k}) = D_{ij}^{-1} F_j^{(0)}(\mathbf{k}), \quad (\text{B10})$$

where

$$D_{ij}^{-1} = \chi(\psi) (\delta_{ij} + \psi \varepsilon_{ijm} \hat{k}_m + \psi^2 k_{ij}), \quad (\text{B11})$$

$$L_{ijmn}^{-1}(\Omega) = \frac{1}{2} \left[B_1 \delta_{im} \delta_{jn} + B_2 k_{ijmn} + B_3 (\varepsilon_{imp} \delta_{jn} + \varepsilon_{jnp} \delta_{im}) \hat{k}_p + B_4 (\delta_{im} k_{jn} + \delta_{jn} k_{im}) + B_5 \varepsilon_{ipm} \varepsilon_{jqn} k_{pq} + B_6 (\varepsilon_{imp} k_{jpn} + \varepsilon_{jnp} k_{ipm}) \right], \quad (\text{B12})$$

$$\tilde{M}_{ij}^F = g e_m \left[(P_{im}(\mathbf{k}) + k_{im}^\lambda) \tilde{F}_j(\mathbf{k}) + (P_{jm}(\mathbf{k}) - k_{jm}^\lambda) \tilde{F}_i(-\mathbf{k}) \right], \quad (\text{B13})$$

$\tilde{F}_i = F_i - F_i^{\Omega=0}$. Here, $\hat{k}_i = k_i/k$, $\chi(\psi) = 1/(1 + \psi^2)$, $\psi = 2\tau(k) \times (\mathbf{k} \cdot \Omega)/k$, $B_1 = 1 + \chi(2\psi)$, $B_2 = B_1 + 2 - 4\chi(\psi)$, $B_3 = 2\psi \chi(2\psi)$, $B_4 = 2\chi(\psi) - B_1$, $B_5 = 2 - B_1$, and $B_6 = 2\psi [\chi(\psi) - \chi(2\psi)]$, see Ref. 64. In Eqs. (B9) and (B10), the operator D_{ij}^{-1} is the inverse of $\delta_{ij} - \tau \tilde{D}_{ij}$ and the operator $L_{ijmn}^{-1}(\Omega)$ is the inverse of $\delta_{im} \delta_{jn} - \tau \tilde{L}_{ijmn}$, where $\tilde{D}_{ij} = 2\varepsilon_{ijp} \Omega_q k_{pq}$ and

$$\tilde{L}_{ijmn} = 2\Omega_q (\varepsilon_{imp} \delta_{jn} + \varepsilon_{jnp} \delta_{im}) k_{pq}. \quad (\text{B14})$$

In Eq. (B9), the operators L_{ijmn}^∇ and L_{ijmn}^λ are given by

$$L_{ijmn}^\nabla = -2\Omega_q (\varepsilon_{imp} \delta_{jn} - \varepsilon_{jnp} \delta_{im}) k_{pq}^\nabla, \quad (\text{B15})$$

$$L_{ijmn}^\lambda = -2\Omega_q \left[(\varepsilon_{imp} \delta_{jn} - \varepsilon_{jnp} \delta_{im}) k_{pq}^\lambda + \frac{2i}{k^2} (\varepsilon_{ilq} \delta_{jn} \lambda_m - \varepsilon_{jilq} \delta_{im} \lambda_n) k_l \right], \quad (\text{B16})$$

where

$$k_{ij}^\nabla = \frac{i}{2k^2} [k_i \nabla_j + k_j \nabla_i - 2k_{ij}(\mathbf{k} \cdot \nabla)], \quad (\text{B17})$$

$$k_{ij}^\lambda = \frac{i}{2k^2} [k_i \lambda_j + k_j \lambda_i - 2k_{ij}(\mathbf{k} \cdot \lambda)]. \quad (\text{B18})$$

In Eqs. (B9) and (B10), we neglected effects $O(\lambda^2, \Lambda^2)$, i.e., they are quadratic in fluid density stratification (described by λ) and inhomogeneity of turbulence (described by $\Lambda = \nabla \langle \mathbf{u}^2 \rangle / \langle \mathbf{u}^2 \rangle$). We also take into account that $L_{ijmn}^{-1} P_{mn}(\mathbf{k}) = P_{ij}(\mathbf{k})$.

We use the following model of the background inhomogeneous and density stratified turbulence $f_{ij}^{(0)}(\mathbf{k}) \equiv \langle U_i(\mathbf{k}_1) U_j(\mathbf{k}_2) \rangle^{(0)}$, which takes into account an anisotropy of turbulence with appearance of rotation

$$f_{ij}^{(0)}(\mathbf{k}) = \frac{E(k) \left[1 + 2k \varepsilon_u \delta(\hat{\mathbf{k}} \cdot \hat{\Omega}) \delta(\hat{\Omega} \cdot \hat{\mathbf{V}}) \right]}{8\pi k^2 (1 + \varepsilon_u)} \times \left[P_{ij}(k) + \frac{i}{k^2} (\tilde{\lambda}_i k_j - \tilde{\lambda}_j k_i) \right] \langle \mathbf{U}^2 \rangle, \quad (\text{B19})$$

and the correlation function $F_i^{(0)}(\mathbf{k}) = \langle s(\mathbf{k}_1) U_i(\mathbf{k}_2) \rangle^{(0)}$ is

$$F_i^{(0)}(\mathbf{k}) = -\tau(k) \tilde{f}_{ij}^{(0)}(\mathbf{k}) \nabla_j \bar{s}, \quad (\text{B20})$$

where the function $\tilde{f}_{ij}^{(0)}(\mathbf{k})$ is given by Eq. (B19) without the terms proportional to $\tilde{\lambda} = (\lambda - \mathbf{V})/2$. Here, we take into account that in

the anelastic approximation the velocity fluctuations $\mathbf{U} = \sqrt{\bar{\rho}} \mathbf{u}'$ satisfy the equation $\nabla \cdot \mathbf{U} = \mathbf{U} \cdot \tilde{\lambda}$, where $\tilde{\lambda} \equiv \lambda/2 = -(\nabla \bar{\rho})/2\bar{\rho}$.

Equation (B19) is derived using symmetry arguments. For instance, density stratification is taken into account in anelastic approximation $\text{div}(\bar{\rho} \mathbf{u}) = 0$ for low-Mach number turbulence. In this case, the derivation of the Reynolds stress in the Fourier space $f_{ij}^{(0)} \equiv \langle U_i(\mathbf{k}_1) U_j(\mathbf{k}_2) \rangle$ for a density-stratified turbulence is described in Sec. 2.2.3 in Ref. 8. The derivation of the Reynolds stress in the Fourier space for an inhomogeneous turbulence is described in Sec. 3.4.3 in Ref. 8. In particular, the large-scale effects caused by stratification λ and inhomogeneous turbulence $\nabla \langle \mathbf{u}^2 \rangle$, satisfy the conditions $\ell_0 \ll H_\rho$ and $\ell_0 \ll L_u$, where H_ρ and L_u is the characteristic scales of the density stratification and inhomogeneity of turbulence, respectively. Therefore, we consider only linear effects in λ and $\nabla \langle \mathbf{u}^2 \rangle$ in Eq. (B19) so that the second-rank tensor $f_{ij}^{(0)}$ is constructed as a linear combination of symmetric tensors, δ_{ij} and k_{ij} , with respect to the indexes i and j , and non-symmetric tensors, $k_i \lambda_j$, $k_j \lambda_i$, and $k_i \nabla_j \langle \mathbf{u}^2 \rangle$, $k_j \nabla_i \langle \mathbf{u}^2 \rangle$. To determine unknown coefficients multiplying by these tensors, we use the following conditions in the derivation of Eq. (B19):

$$\langle \mathbf{u}^2 \rangle = \int f_{ii}^{(0)}(\mathbf{k}, \mathbf{K}) \exp(i\mathbf{K} \cdot \mathbf{R}) d\mathbf{k} d\mathbf{K}, \quad (\text{B21})$$

$$\langle (\text{div} \mathbf{u})^2 \rangle = \int k_i k_j f_{ij}^{(0)}(\mathbf{k}, \mathbf{K}) \exp(i\mathbf{K} \cdot \mathbf{R}) d\mathbf{k} d\mathbf{K}. \quad (\text{B22})$$

The anisotropy of turbulence is caused by a fast rotation. The anisotropic turbulence can be described as a combination of a three-dimensional isotropic turbulence and two-dimensional turbulence in the plane perpendicular to the rotational axis. The degree of anisotropy ε_u is defined as the ratio of turbulent kinetic energies of two-dimensional to three-dimensional motions. The parameter ε_u is non-zero only for a fast rotation $\Omega_* \gg 1$.

In Eq. (B19), $\delta(x)$ is the Dirac delta function. For a fast rotation λ is perpendicular to Ω . The turbulent correlation time in the \mathbf{k} space is $\tau(k) = 2\tau_0 \tilde{\tau}(k)$, where $\tilde{\tau}(k) = (k/k_0)^{1-q}$. We assume that the background turbulence is of Kolmogorov type with constant flux of energy over the spectrum, i.e., the kinetic energy spectrum function for the range of wave numbers $k_0 < k < k_\nu$ is $E(k) = -d\tilde{\tau}(k)/dk$, the function $\tilde{\tau}(k) = (k/k_0)^{1-q}$ with $1 < q < 3$ being the exponent of the kinetic energy spectrum ($q = 5/3$ for a Kolmogorov spectrum). Here, $k_\nu = 1/\ell_\nu$ is the wave number based on the viscous scale ℓ_ν , and $k_0 = 1/\ell_0 \ll k_\nu$, where ℓ_0 is the integral (energy containing) scale of turbulent motions.

Note that a direct effect of rotation on turbulence is described self-consistently by Eqs. (B1) and (B2). The kinetic helicity is produced by the natural way due to the combined effect of uniform rotation and density stratification or inhomogeneity of turbulence. The fast rotation is included in the background turbulence only via the term proportional to ε_u to take into account appearance of strong anisotropy of background turbulence caused by the fast rotation. This is ‘‘indirect’’ effect of transition from three-dimensional nearly isotropic turbulence for slow rotation to a strongly anisotropic nearly two-dimensional turbulence.

Using Eqs. (B9) and (B10), we obtain $f_{ij}^{(\Omega, a)}(\mathbf{k}) = L_{ijmn}^{-1} f_{mn}^{(0)}(\mathbf{k})$ and $F_i^{(\Omega)}(\mathbf{k}) = D_{ij}^{-1} F_j^{(0)}(\mathbf{k})$ as

$$f_{ij}^{(\Omega, a)}(\mathbf{k}) = \frac{E(k) \left[1 + 2k \varepsilon_u \delta(\hat{\mathbf{k}} \cdot \hat{\boldsymbol{\Omega}}) \delta(\hat{\boldsymbol{\Omega}} \cdot \hat{\mathbf{V}}) \right]}{8\pi k^2 (1 + \varepsilon_u)} \left[P_{ij}(k) + \frac{i}{k} \chi(\psi) \left[\tilde{\lambda}_i \hat{k}_j - \tilde{\lambda}_j \hat{k}_i + \psi \tilde{\lambda}_n (\varepsilon_{inp} k_{jp} - \varepsilon_{jnp} k_{ip}) \right] \right] \langle \mathbf{U}^2 \rangle, \tag{B23}$$

$$F_i^{(\Omega)}(\mathbf{k}) = -\frac{\tau(k) E(k) \left[1 + 2k \varepsilon_u \delta(\hat{\mathbf{k}} \cdot \hat{\boldsymbol{\Omega}}) \right]}{8\pi k^2 (1 + \varepsilon_u)} (\nabla_j \bar{S}) \times \chi(\psi) \left[P_{ij}(k) + \psi \varepsilon_{ijs} \hat{k}_s \right] \langle \mathbf{U}^2 \rangle. \tag{B24}$$

Using Eqs. (B24) and (27)–(28), we determine $\langle \tau u_i(\mathbf{x}) [\nabla^2 \theta(\mathbf{x})] \rangle$ as

$$\langle \tau u_i(\mathbf{x}) [\nabla^2 \theta(\mathbf{x})] \rangle = \frac{1}{1 + \varepsilon_u} \left[2A_1^{(-1)}(\Omega_*) \delta_{ij} + (A_2^{(-1)}(\Omega_*) + \frac{\varepsilon_u}{2} \ln \text{Re}) (\delta_{ij} - \hat{\Omega}_{ij}) + \hat{\Omega}_m \varepsilon_{ijm} \Omega_* A_3^{(0)}(\Omega_*) \right] \nabla_j \ln(\bar{T} \bar{P}^{1/\gamma-1}). \tag{B25}$$

The functions $A_n^{(m)}(\Omega_*)$ are given in Appendix C.

APPENDIX C: THE IDENTITIES USED FOR THE INTEGRATION IN THE k SPACE

To integrate over the angles in the \mathbf{k} space we used the following identities:

$$\bar{I}_{ij}(a) = \int \frac{k_{ij} \sin \theta}{1 + a \cos^2 \theta} d\theta d\varphi = \bar{A}_1(a) \delta_{ij} + \bar{A}_2(a) \Omega_{ij}, \tag{C1}$$

$$\bar{I}_{ijmn}(a) = \int \frac{k_{ijmn} \sin \theta}{1 + a \cos^2 \theta} d\theta d\varphi = \bar{C}_1 \Delta_{ijmn} + \bar{C}_2 \Omega_{ijmn} + \bar{C}_3 \Delta_{ijmn}^{(\Omega)}, \tag{C2}$$

where $\Omega_{ij} = \hat{\Omega}_i \hat{\Omega}_j$, and $\Omega_{ijmn} = \Omega_{ij} \Omega_{mn}$,

$$\Delta_{ijmn} = \delta_{ij} \delta_{mn} + \delta_{im} \delta_{jn} + \delta_{in} \delta_{jm}, \tag{C3}$$

$$\Delta_{ijmn}^{(\Omega)} = \delta_{ij} \Omega_{mn} + \delta_{im} \Omega_{jn} + \delta_{in} \Omega_{jm} + \delta_{jm} \Omega_{in} + \delta_{jn} \Omega_{im} + \delta_{mn} \Omega_{ij}, \tag{C4}$$

and the functions $\bar{A}_k(a)$ and $\bar{C}_k(a)$ are given by

$$\bar{A}_1(a) = \frac{2\pi}{a} \left[(a+1) \frac{\arctan(\sqrt{a})}{\sqrt{a}} - 1 \right], \tag{C5}$$

$$\bar{A}_2(a) = -\frac{2\pi}{a} \left[(a+3) \frac{\arctan(\sqrt{a})}{\sqrt{a}} - 3 \right], \tag{C6}$$

$$\bar{C}_1(a) = \frac{\pi}{2a^2} \left[(a+1)^2 \frac{\arctan(\sqrt{a})}{\sqrt{a}} - \frac{5a}{3} - 1 \right], \tag{C7}$$

$$\bar{C}_2(a) = \frac{\pi}{2a^2} \left[(3a^2 + 30a + 35) \frac{\arctan(\sqrt{a})}{\sqrt{a}} - \frac{55a}{3} - 35 \right], \tag{C8}$$

$$\bar{C}_3(a) = -\frac{\pi}{2a^2} \left[(a^2 + 6a + 5) \frac{\arctan(\sqrt{a})}{\sqrt{a}} - \frac{13a}{3} - 5 \right]. \tag{C9}$$

Note that $\bar{A}_1 = 5\bar{C}_1 + \bar{C}_3$ and $\bar{A}_2 = \bar{C}_2 + 7\bar{C}_3$.

We introduce also the function $\bar{A}_3(a) = \bar{A}_1(a) + \bar{A}_2(a)$ and $\bar{C}_4(a) = \bar{C}_1(a) + \bar{C}_3(a)$

$$\bar{A}_3(a) = \frac{4\pi}{a} \left[1 - \frac{\arctan(\sqrt{a})}{\sqrt{a}} \right]. \tag{C10}$$

$$\bar{C}_4(a) = \frac{2\pi}{a^2} \left[1 + \frac{2a}{3} - (a+1) \frac{\arctan(\sqrt{a})}{\sqrt{a}} \right]. \tag{C11}$$

These functions for $a \ll 1$ are given by

$$\bar{A}_1(a) = \frac{4\pi}{3} \left(1 - \frac{a}{5} \right), \quad \bar{A}_2(a) \sim -\frac{8\pi}{15} a, \tag{C12}$$

$$\bar{C}_1(a) \sim \frac{4\pi}{15} \left(1 - \frac{a}{7} \right), \quad \bar{C}_2(a) \sim \frac{32\pi}{315} a^2, \tag{C13}$$

$$\bar{C}_3(a) \sim -\frac{8\pi}{105} a, \quad \bar{C}_4(a) \sim \frac{4\pi}{15} \left(1 - \frac{3a}{7} \right). \tag{C14}$$

These functions for $a \gg 1$ are given by

$$\bar{A}_1(a) \sim \frac{\pi^2}{\sqrt{a}}, \quad \bar{A}_2(a) \sim -\frac{\pi^2}{\sqrt{a}}, \tag{C15}$$

$$\bar{C}_1(a) \sim \frac{\pi^2}{4\sqrt{a}} - \frac{4\pi}{3a}, \quad \bar{C}_2(a) \sim \frac{3\pi^2}{4\sqrt{a}}, \tag{C16}$$

$$\bar{C}_3(a) \sim -\frac{\pi^2}{4\sqrt{a}} + \frac{8\pi}{3a}, \quad \bar{C}_4(a) \sim \frac{4\pi}{3a} - \frac{\pi^2}{a^{3/2}}. \tag{C17}$$

Now, we calculate the following functions:

$$A_k^{(p)}(\Omega_*) = \frac{3}{4\pi \Omega_*^{p+1}} \int_0^{\Omega_*} Y^p \bar{A}_k(Y^2) dY, \tag{C18}$$

$$C_k^{(p)}(\Omega_*) = \frac{15}{4\pi \Omega_*^{p+1}} \int_0^{\Omega_*} Y^p \bar{C}_k(Y^2) dY, \tag{C19}$$

where $p \geq 0$, and

$$A_k^{(-1)}(\Omega_*) = \frac{3}{4\pi} \int_{\Omega_* \text{Re}^{-1/2}}^{\Omega_*} Y^{-1} \bar{A}_k(Y^2) dY, \tag{C20}$$

where $\Omega_* = 4\Omega \tau_0$, $a = [\Omega_* \bar{\tau}(k)]^2 = Y^2$ and $\bar{\tau}_\nu = \text{Re}^{-1/2}$. The integration yields

$$A_1^{(1)}(Z) = \frac{3}{2} \left[\frac{\arctan Z}{Z} \left(1 - \frac{1}{Z^2} \right) + \frac{1}{Z^2} [1 - \ln(1 + Z^2)] \right], \tag{C21}$$

$$A_2^{(1)}(Z) = -\frac{3}{2} \left[\frac{\arctan Z}{Z} \left(1 - \frac{3}{Z^2} \right) + \frac{1}{Z^2} [3 - 2 \ln(1 + Z^2)] \right], \tag{C22}$$

$$A_1^{(2)}(Z) = \frac{3}{4} \left[\frac{\arctan Z}{Z} \left(1 + \frac{1}{Z^2} \right) - \frac{3}{Z^2} + \frac{2}{Z^3} S(Z) \right], \tag{C23}$$

$$A_2^{(2)}(Z) = -\frac{3}{4} \left[\frac{\arctan Z}{Z} \left(1 + \frac{1}{Z^2} \right) - \frac{7}{Z^2} + \frac{6}{Z^3} S(Z) \right], \tag{C24}$$

$$A_3^{(2)}(Z) = \frac{3}{Z^3} [Z - S(Z)], \tag{C25}$$

$$A_1^{(0)}(Z) = -\frac{3}{4} \left[\arctan Z \left(1 + \frac{1}{Z^2} \right) - \frac{1}{Z} - 2S(Z) \right], \quad (C26)$$

$$A_2^{(0)}(Z) = \frac{9}{4} \left[\arctan Z \left(1 + \frac{1}{Z^2} \right) - \frac{1}{Z} - \frac{2}{3} S(Z) \right], \quad (C27)$$

$$A_3^{(0)}(Z) = \frac{3}{2} \left[\left(1 + \frac{1}{Z^2} \right) \arctan Z - \frac{1}{Z} \right], \quad (C28)$$

$$A_1^{(-1)}(Z) = \frac{1}{2} \left[\frac{8}{3} - \frac{\arctan Z}{Z} \left(3 + \frac{1}{Z^2} \right) + \frac{1}{Z^2} + \ln \left(\frac{\text{Re}}{1 + Z^2} \right) \right], \quad (C29)$$

$$A_2^{(-1)}(Z) = \frac{3}{2} \left[\frac{\arctan Z}{Z} \left(1 + \frac{1}{Z^2} \right) - \frac{1}{Z^2} - \frac{2}{3} \right], \quad (C30)$$

$$A_3^{(-1)}(Z) = \frac{1}{3} \left[1 + \frac{3}{Z^2} \left(\frac{\arctan Z}{Z} - 1 \right) \right] + \frac{1}{2} \ln \left(\frac{\text{Re}}{1 + Z^2} \right), \quad (C31)$$

$$C_1^{(2)}(Z) = \frac{15}{16} \left[\frac{\arctan Z}{Z} \left(1 - \frac{1}{Z^4} \right) - \frac{13}{3Z^2} + \frac{1}{Z^4} + \frac{4S(Z)}{Z^3} \right], \quad (C32)$$

$$C_4^{(2)}(Z) = \frac{15}{4Z^3} \left[\arctan Z \left(1 + \frac{1}{Z^2} \right) - \frac{1}{Z} + \frac{4Z}{3} - 2S(Z) \right], \quad (C33)$$

$$C_1^{(3)}(Z) = \frac{15}{8Z^4} \left[\frac{\arctan Z}{Z} \left(\frac{Z^4}{3} + 2Z^2 - 1 \right) - Z^2 + 1 - \frac{4}{3} \ln(1 + Z^2) \right], \quad (C34)$$

$$C_1^{(0)}(Z) = -\frac{15}{32} \left[\arctan Z \left(3 + \frac{4}{Z^2} + \frac{1}{Z^4} \right) - \frac{11}{3Z} - \frac{1}{Z^3} - 4S(Z) \right], \quad (C35)$$

$$C_4^{(0)}(Z) = \frac{15}{8} \left[\arctan Z \left(1 + \frac{1}{Z^2} \right)^2 - \frac{5}{3Z} - \frac{1}{Z^3} \right], \quad (C36)$$

where $S(Z) = \int_0^Z [\arctan(Y)/Y] dY$. These functions for $Z \ll 1$ are given by

$$A_1^{(1)}(Z) \sim \frac{1}{2} \left(1 - \frac{Z^2}{10} \right), \quad A_2^{(1)}(Z) \sim -\frac{Z^2}{10} + \frac{2Z^4}{35},$$

$$A_3^{(1)}(Z) \sim \frac{1}{2} \left(1 - \frac{3Z^2}{10} \right), \quad A_3^{(2)}(Z) \sim \frac{1}{3} \left(1 - \frac{9Z^2}{25} \right),$$

$$A_1^{(2)}(Z) \sim \frac{1}{3} \left(1 - \frac{3Z^2}{25} \right), \quad A_1^{(0)}(Z) \sim Z \left(1 - \frac{Z^2}{15} \right),$$

$$A_2^{(2)}(Z) \sim -\frac{3Z^2}{20} \left(1 - \frac{4Z^2}{7} \right), \quad A_2^{(0)}(Z) \sim -\frac{2Z^3}{15},$$

$$A_3^{(0)}(Z) \sim Z \left(1 - \frac{Z^2}{5} \right), \quad A_2^{(-1)}(Z) \sim -\frac{Z^2}{5},$$

$$A_1^{(-1)}(Z) \sim \frac{1}{2} \left(\ln \text{Re} - \frac{Z^2}{5} \right),$$

$$A_3^{(-1)}(Z) \sim \frac{1}{2} \left(\ln \text{Re} + \frac{Z^2}{5} \right),$$

$$C_1^{(2)}(Z) \sim \frac{1}{3} \left(1 - \frac{3Z^2}{35} \right), \quad C_4^{(2)}(Z) \sim \frac{1}{3} \left(1 - \frac{9Z^2}{35} \right),$$

$$C_1^{(3)}(Z) \sim \frac{1}{4} \left(1 - \frac{2Z^2}{21} \right), \quad C_1^{(0)}(Z) \sim Z,$$

$$C_4^{(0)}(Z) \sim Z \left(1 - \frac{Z^2}{7} \right).$$

These functions for $Z \gg 1$ are given by

$$A_1^{(1)}(Z) \sim \frac{3\pi}{4Z} - \frac{3 \ln Z}{Z^2}, \quad A_2^{(1)}(Z) \sim -\frac{3\pi}{4Z} + \frac{6 \ln Z}{Z^2},$$

$$A_3^{(1)}(Z) \sim \frac{3 \ln Z}{Z^2}, \quad A_3^{(2)}(Z) \sim \frac{3}{Z^2},$$

$$A_1^{(2)}(Z) \sim \frac{3\pi}{8Z} \left(1 - \frac{6}{\pi Z} \right), \quad A_2^{(2)}(Z) \sim -\frac{3\pi}{8Z} \left(1 - \frac{14}{\pi Z} \right),$$

$$A_1^{(0)}(Z) \sim \frac{3\pi}{4} \left(\ln Z - \frac{1}{2} \right), \quad A_2^{(0)}(Z) \sim -\frac{3\pi}{4} \ln Z,$$

$$A_3^{(0)}(Z) \sim \frac{3}{4} \left(\pi - \frac{2}{Z} \right), \quad A_2^{(-1)}(Z) \sim \frac{3}{4} \left(\frac{\pi}{Z} - \frac{4}{3} \right),$$

$$C_1^{(2)}(Z) \sim \frac{15\pi}{32Z}, \quad C_1^{(3)}(Z) \sim \frac{5\pi}{16Z}, \quad C_4^{(2)}(Z) \sim \frac{5}{Z^2},$$

$$C_1^{(0)}(Z) \sim \frac{15\pi}{16} \left(\ln Z - \frac{3}{4} \right), \quad C_4^{(0)}(Z) \sim -\frac{5}{Z} + \frac{15\pi}{16}.$$

and when $1 \ll Z^2 \ll \text{Re}$, the function

$$A_1^{(-1)}(Z) \sim \frac{1}{2} \left[\ln \left(\frac{\text{Re}}{Z^2} \right) + \frac{8}{3} \right],$$

$$A_3^{(-1)}(Z) \sim \frac{1}{2} \left[\ln \left(\frac{\text{Re}}{Z^2} \right) + \frac{2}{3} \right].$$

To integrate over the angles in \mathbf{k} -space for anisotropic part of turbulence, we use the following integrals:

$$\int k_{ij}^+ d\varphi = \pi \delta_{ij}^{(2)}, \quad \int k_{ijmn}^+ d\varphi = \frac{\pi}{4} \Delta_{ijmn}^{(2)}, \quad (C37)$$

where $\delta_{ij}^{(2)} \equiv P_{ij}(\Omega) = \delta_{ij} - \Omega_{ij}$ and $\Delta_{ijmn}^{(2)} = P_{ij}(\Omega)P_{mn}(\Omega) + P_{im}(\Omega)P_{jn}(\Omega) + P_{in}(\Omega)P_{jm}(\Omega)$.

REFERENCES

- ¹S. Twomey, *Atmospheric Aerosols* (Elsevier Scientific Publication Comp., Amsterdam, 1977).
- ²G. T. Csanady, *Turbulent Diffusion in the Environment* (Reidel, Dordrecht, 1980).
- ³Y. B. Zeldovich, A. A. Ruzmaikin, and D. D. Sokoloff, *The Almighty Chance* (Word Scientific Publ., Singapore, 1990).
- ⁴A. K. Blackadar, *Turbulence and Diffusion in the Atmosphere* (Springer, Berlin, 1997).
- ⁵J. H. Seinfeld and S. N. Pandis, *Atmospheric Chemistry and Physics. From Air Pollution to Climate Change*, 2nd ed. (John Wiley & Sons, New York, 2006).
- ⁶L. I. Zaichik, V. M. Alipchenkov, and E. G. Sinaiski, *Particles in Turbulent Flows* (John Wiley & Sons, New York, 2008).
- ⁷C. T. Crowe, J. D. Schwarzkopf, M. Sommerfeld, and Y. Tsuji, *Multiphase Flows with Droplets and Particles*, 2nd ed. (CRC Press LLC, New York, 2011).
- ⁸I. Rogachevskii, *Introduction to Turbulent Transport of Particles, Temperature and Magnetic Fields* (Cambridge University Press, Cambridge, UK, 2021).
- ⁹L. S. Hodgson and A. Brandenburg, "Turbulence effects in planetesimal formation," *Astron. Astrophys.* **330**, 1169–1174 (1998).
- ¹⁰T. Elperin, N. Kleorin, and I. Rogachevskii, "Dynamics of particles advected by fast rotating turbulent fluid flow: Fluctuations and large-scale structures," *Phys. Rev. Lett.* **81**, 2898 (1998).
- ¹¹L. Pan, P. Padoan, J. Scalo, A. G. Kritsuk, and M. L. Norman, "Turbulent clustering of protoplanetary dust and planetesimal formation," *Astrophys. J.* **740**, 6 (2011).
- ¹²A. Hubbard, "Turbulent thermal diffusion: A way to concentrate dust in protoplanetary discs," *Mon. Not. R. Astron. Soc.* **456**, 3079–3089 (2016).

- ¹³P. F. Hopkins, "A simple phenomenological model for grain clustering in turbulence," *Mon. Not. R. Astron. Soc.* **455**, 89–111 (2016).
- ¹⁴P. F. Hopkins, "Jumping the gap: The formation conditions and mass function of 'pebble-pile' planetesimals," *Mon. Not. R. Astron. Soc.* **456**, 2383–2405 (2016).
- ¹⁵H. J. Lugt, *Vortex Flow in Nature and Technology* (Wiley, New York, 1983).
- ¹⁶M. Caporaloni, F. Tampieri, F. Trombetti, and O. Vittori, "Transfer of particles in nonisotropic air turbulence," *J. Atmos. Sci.* **32**, 565 (1975).
- ¹⁷M. Reeks, "The transport of discrete particle in inhomogeneous turbulence," *J. Aerosol Sci.* **14**, 729 (1983).
- ¹⁸A. Guha, "Transport and deposition of particles in turbulent and laminar flow," *Annu. Rev. Fluid Mech.* **40**, 311 (2008).
- ¹⁹D. Mitra, N. E. L. Haugen, and I. Rogachevskii, "Turbophoresis in forced inhomogeneous turbulence," *Euro. Phys. J. Plus* **133**, 35 (2018).
- ²⁰T. Elperin, N. Kleeorin, and I. Rogachevskii, "Turbulent thermal diffusion of small inertial particles," *Phys. Rev. Lett.* **76**, 224 (1996).
- ²¹T. Elperin, N. Kleeorin, and I. Rogachevskii, "Turbulent barodiffusion, turbulent thermal diffusion and large-scale instability in gases," *Phys. Rev. E* **55**, 2713 (1997).
- ²²T. Elperin, N. Kleeorin, and I. Rogachevskii, "Formation of inhomogeneities in two-phase low-Mach-number compressible turbulent flows," *Int. J. Multiphase Flow* **24**, 1163 (1999).
- ²³T. Elperin, N. Kleeorin, I. Rogachevskii, and D. Sokoloff, "Passive scalar transport in a random flow with a finite renewal time: Mean-field equations," *Phys. Rev. E* **61**, 2617 (2000).
- ²⁴T. Elperin, N. Kleeorin, I. Rogachevskii, and D. Sokoloff, "Mean-field theory for a passive scalar advected by a turbulent velocity field with a random renewal time," *Phys. Rev. E* **64**, 026304 (2001).
- ²⁵R. V. R. Pandya and F. Mashayek, "Turbulent thermal diffusion and barodiffusion of passive scalar and dispersed phase of particles in turbulent flows," *Phys. Rev. Lett.* **88**, 044501 (2002).
- ²⁶M. W. Reeks, "On model equations for particle dispersion in inhomogeneous turbulence," *Int. J. Multiph. Flow* **31**, 93 (2005).
- ²⁷G. Amir, N. Bar, A. Eidelman, T. Elperin, N. Kleeorin, and I. Rogachevskii, "Turbulent thermal diffusion in strongly stratified turbulence: Theory and experiments," *Phys. Rev. Fluids* **2**, 064605 (2017).
- ²⁸N. E. L. Haugen, N. Kleeorin, I. Rogachevskii, and A. Brandenburg, "Detection of turbulent thermal diffusion of particles in numerical simulations," *Phys. Fluids* **24**, 075106 (2012).
- ²⁹A. Brandenburg, K.-H. Rädler, and K. Kemel, "Mean-field transport in stratified and/or rotating turbulence," *Astron. Astrophys.* **539**, A35 (2012).
- ³⁰I. Rogachevskii, N. Kleeorin, and A. Brandenburg, "Compressibility in turbulent magnetohydrodynamics and passive scalar transport: Mean-field theory," *J. Plasma Phys.* **84**, 735840502 (2018).
- ³¹J. Buchholz, A. Eidelman, T. Elperin, G. Grünefeld, N. Kleeorin, A. Krein, and I. Rogachevskii, "Experimental study of turbulent thermal diffusion in oscillating grids turbulence," *Exp. Fluids* **36**, 879 (2004).
- ³²A. Eidelman, T. Elperin, N. Kleeorin, I. Rogachevskii, and I. Sapir-Kitiraie, "Turbulent thermal diffusion in a multi-fan turbulence generator with the imposed mean temperature gradient," *Exp. Fluids* **40**, 744 (2006).
- ³³E. Elmakies, O. Shildkrot, N. Kleeorin, A. Levy, I. Rogachevskii, and A. Eidelman, "Experimental study of turbulent thermal diffusion of particles in inhomogeneous and anisotropic turbulence," *Phys. Fluids* **34**, 055125 (2022).
- ³⁴I. Shimberg, O. Shriki, O. Shildkrot, N. Kleeorin, A. Levy, and I. Rogachevskii, "Experimental study of turbulent transport of nanoparticles in convective turbulence," *Phys. Fluids* **34**, 055126 (2022).
- ³⁵E. Elmakies, O. Shildkrot, N. Kleeorin, A. Levy, and I. Rogachevskii, "Experimental study of turbulent thermal diffusion of particles in an inhomogeneous forced convective turbulence," *Phys. Fluids* **35**, 095123 (2023).
- ³⁶M. Sofiev, V. Sofieva, T. Elperin, N. Kleeorin, I. Rogachevskii, and S. S. Zilitinkevich, "Turbulent diffusion and turbulent thermal diffusion of aerosols in stratified atmospheric flows," *J. Geophys. Res.* **114**, D18209, <https://doi.org/10.48550/arXiv.0908.2762> (2009).
- ³⁷T. Elperin, N. Kleeorin, M. Podolak, and I. Rogachevskii, "A mechanism for the formation of aerosol concentrations in the atmosphere of Titan," *Planet. Space Sci.* **45**, 923–929 (1997).
- ³⁸M. R. Maxey, "The gravitational settling of aerosol particles in homogeneous turbulence and random flow field," *J. Fluid Mech.* **174**, 441 (1987).
- ³⁹I. Rogachevskii and N. Kleeorin, "Mean-field theory of differential rotation in density stratified turbulent convection," *J. Plasma Phys.* **84**, 735840201 (2018).
- ⁴⁰I. Rogachevskii and N. Kleeorin, "Generation of a large-scale vorticity in a fast rotating density stratified turbulence or turbulent convection," *Phys. Rev. E* **100**, 063101 (2019).
- ⁴¹P. H. Roberts and A. M. Soward, "A unified approach to mean field electrodynamics," *Astron. Nachr.* **296**, 49 (1975).
- ⁴²S. A. Orszag, "Analytical theories of turbulence," *J. Fluid Mech.* **41**, 363 (1970).
- ⁴³A. Pouquet, U. Frisch, and J. Leorat, "Strong MHD helical turbulence and the nonlinear dynamo effect," *J. Fluid Mech.* **77**, 321 (1976).
- ⁴⁴N. Kleeorin, I. Rogachevskii, and A. Ruzmaikin, "Magnetic force reversal and instability in a plasma with advanced magnetohydrodynamic turbulence," *Zh. Eksp. Teor. Fiz.* **97**, 1555 (1990). [*Sov. Phys. JETP* **70** 878 (1990)].
- ⁴⁵P. J. Käpylä, M. J. Mantere, and T. Hackman, "Starspots due to large-scale vortices in rotating turbulent convection," *Astrophys. J.* **742**, 34 (2011).
- ⁴⁶M. J. Mantere, P. J. Käpylä, and T. Hackman, "Dependence of the large-scale vortex instability on latitude, stratification, and domain size," *Astron. Nachr.* **332**, 876 (2011).
- ⁴⁷A. Brandenburg, P. J. Käpylä, and A. Mohammed, "Non-Fickian diffusion and tau approximation from numerical turbulence," *Phys. Fluids* **16**, 1020 (2004).
- ⁴⁸T. Elperin, N. Kleeorin, I. Rogachevskii, and S. S. Zilitinkevich, "Formation of large-scale semi-organized structures in turbulent convection," *Phys. Rev. E* **66**, 066305 (2002).
- ⁴⁹T. Elperin, N. Kleeorin, I. Rogachevskii, and S. S. Zilitinkevich, "Tangling turbulence and semi-organized structures in convective boundary layers," *Boundary-Layer Meteorol.* **119**, 449 (2006).
- ⁵⁰J. L. Lumley, "Rational approach to relations between motions of differing scales in turbulent flows," *Phys. Fluids* **10**, 1405 (1967).
- ⁵¹T. Ishihara, K. Yoshida, and Y. Kaneda, "Anisotropic velocity correlation spectrum at small scales in a homogeneous turbulent shear flow," *Phys. Rev. Lett.* **88**, 154501 (2002).
- ⁵²S. G. Saddoughi and S. V. Veeravalli, "Local isotropy in turbulent boundary layers at high Reynolds number," *J. Fluid Mech.* **268**, 333 (1994).
- ⁵³J. C. Wyngaard and O. R. Cote, "Cospectral similarity in the atmospheric surface layer," *Q. J. R. Meteorol. Soc.* **98**, 590 (1972).
- ⁵⁴A. Brandenburg, O. Gressel, P. J. Käpylä, N. Kleeorin, M. J. Mantere, and I. Rogachevskii, "New scaling for the alpha effect in slowly rotating turbulence," *Astrophys. J.* **762**, 127 (2013).
- ⁵⁵I. Rogachevskii, O. Ruchayskiy, A. Boyarsky, J. Fröhlich, N. Kleeorin, A. Brandenburg, and J. Schober, "Laminar and turbulent dynamos in chiral magnetohydrodynamics. I. Theory," *Astrophys. J.* **846**, 153 (2017).
- ⁵⁶A. Brandenburg, J. Schober, I. Rogachevskii, T. Kahniashvili, A. Boyarsky, J. Fröhlich, O. Ruchayskiy, and N. Kleeorin, "The turbulent chiral magnetic cascade in the early universe," *Astrophys. J. Lett.* **845**, L21 (2017).
- ⁵⁷J. Schober, I. Rogachevskii, A. Brandenburg, A. Boyarsky, J. Fröhlich, O. Ruchayskiy, and N. Kleeorin, "Laminar and turbulent dynamos in chiral magnetohydrodynamics. II. Simulations," *Astrophys. J.* **858**, 124 (2018).
- ⁵⁸J. Schober, I. Rogachevskii, and A. Brandenburg, "Production of a chiral magnetic anomaly with emerging turbulence and mean-field dynamo action," *Phys. Rev. Lett.* **128**, 065002 (2022).
- ⁵⁹J. Schober, I. Rogachevskii, and A. Brandenburg, "Chiral anomaly and dynamos from inhomogeneous chemical potential fluctuations," *Phys. Rev. Lett.* **132**, 065101 (2024).
- ⁶⁰A. Brandenburg, K. Kemel, N. Kleeorin, D. Mitra, and I. Rogachevskii, "Detection of negative effective magnetic pressure instability in turbulence simulations," *Astrophys. J.* **740**, L50 (2011).
- ⁶¹A. Brandenburg, I. Rogachevskii, and N. Kleeorin, "Magnetic concentrations in stratified turbulence: The negative effective magnetic pressure instability," *New J. Phys.* **18**, 125011 (2016).
- ⁶²P. Chassaing, R. A. Antonia, F. Anselmetti, L. Joly, and S. Sarkar, *Variable Density Fluid Turbulence* (Kluwer Academic, Dordrecht, 2002).
- ⁶³T. Birnstiel, C. P. Dullemond, and F. Brauer, "Gas- and dust evolution in protoplanetary disks," *Astron. Astrophys.* **513**, A79 (2010).
- ⁶⁴T. Elperin, I. Golubev, N. Kleeorin, and I. Rogachevskii, "Excitation of large-scale inertial waves in a rotating inhomogeneous turbulence," *Phys. Rev. E* **71**, 036302 (2005).